Transition Metal Complexes with Sterically Demanding Ligands, 3.[1] Synthetic Access to Square-Planar Terdentate Pyridine−Diimine Rhodium(I) and Iridium(I) Methyl Complexes: Successful Detour via Reactive Triflate and Methoxide Complexes

Stefan Nückel and Peter Burger*

Anorganisch-chemisches Institut der Universität Zürich, Winterthurerstrasse 190, CH-8057 Zürich, Switzerland

Received March 8, 2001

The synthesis of novel square-planar, terdentate, aryl-substituted pyridine−diimine Rh(I) and Ir(I) chloro complexes from the free ligands and the bis(μ-chloro) ethylene-bridged dimers $[(C_2H_4)RhIrCl]_2$ is reported. Since attempts to achieve direct conversion to the corresponding hydride and methyl complexes through metathesis of the chloro ligand in these compounds were unsuccessful, synthetic access to more reactive methoxy- and triflate-substituted starting materials was developed. The methoxy and triflate complexes could be successfully converted to the Rh(I) η^2-BH_4 and Rh,Ir(I) methyl complexes. The structure and bonding and thermodynamics of the methoxy and η^2-BH_4 species were analyzed by DFT methods. X-ray crystal structures of selected Rh,Ir(I,III) representatives are reported.

Introduction

Square-planar (sq-pl) Rh(I) complexes play an important role as precursors and intermediates in hydrogenation, hydrosilylation, and hydroformylation catalysis and the Monsanto acetic acid process.[2] While the chemistry of these compounds is in principle well explored, there is still room for surprises. In particular, Milstein's group reported recently on exciting intramolecular Rh-mediated C−C and C−O cleavage reactions.[3−8] In their studies, terdentate cyclometalated bis-phosphine donors (P,C,P) were applied. Similar reactivity patterns were observed for the related 1,3-(dimethylamino)phenyl N,C,N pincer ligands (1,3-$(NMe_2)_2$-C_6H_3), which were introduced and used with success by van Koten et al.[9,10] Recently, we reported on our unsuccessful attempts to achieve metal complexation of a related 1,3-diimine−phenyl "ligand" (N,C,N), which we attributed to a potentially difficult C−H activation step.[1] We have therefore switched to the corresponding pyridine−diimine (N,N,N) ligand system, which has been used with great success in the synthesis and catalysis of transition-metal complexes.[11−23] The groups of Vrieze and van Leeuwen have reported, for instance, on the reversible coordination of O_2 to sq-pl pyridine−diimine Rh(I) chloro complexes to give the corresponding peroxo Rh(III) compounds.[19] In context with our longstanding interest in aerobic oxidation catalysis,[24] this prompted us to investigate the corresponding novel Rh(I) and Ir(I) alkyl and hydride complexes, for which no synthesis had been published previously. Herein, we describe the synthetic detour we had to follow to achieve this goal and report on the sq-pl pyridine−diimine Rh(I) triflate and Rh(I),Ir(I) methoxide starting materials, which were developed in the course of these investigations.

(1) Nückel, S.; Burger, P. *Organometallics* **2000**, *19*, 3305.
(2) Cornils, B., Herrmann, W. A., Eds. *Applied Homgeneous Catalysis with Organometallic Compounds*; Wiley-VCH: Weinheim, Germany, 2000.
(3) van der Boom, M. E.; Liou, S.-Y.; Ben-David, Y.; Gozin, M.; Milstein, D. *J. Am. Chem. Soc.* **1998**, *120*, 13415.
(4) van der Boom, M. E.; Liou, S.-Y.; Ben-David, Y.; Vigalok, A.; Milstein, D. *Angew. Chem., Int. Ed.* **1997**, *36*, 625.
(5) Sundermann, A.; Uzan, O.; Milstein, D.; Martin, J. M. L. *J. Am. Chem. Soc.* **2000**, *122*, 7095.
(6) Gozin, M.; Weisman, A.; Ben-David, Y.; Milstein, D. *Nature* **1993**, *364*, 699.
(7) Gandelman, M.; Vigalok, A.; Konstantinovski, L.; Milstein, D. *J. Am. Chem. Soc.* **2000**, *122*, 9848.
(8) Blum, O.; Milstein, D. *J. Am. Chem. Soc.* **1995**, *117*, 4582.
(9) Rietveld, M. H. P.; Grove, D. M.; van Koten, G. *New J. Chem.* **1997**, *21*, 751.
(10) Albrecht, M.; Gossagem, R. A.; Spek, A. L.; van Koten, G. *J. Am. Chem. Soc.* **1999**, *121*, 11898.
(11) Alyea, E. C.; Merrel, P. H. *Inorg. Met.-Org. Chem.* **1974**, *4*, 535.
(12) Bruin, B.; Bill, E.; Bothe, E.; Weyhermüller, T.; Wieghardt, K. *Inorg. Chem.* **2000**, *39*, 2936.
(13) Bianchini, C.; Lee, H. M. *Organometallics* **2000**, *19*, 1833.
(14) Britovsek, G. J. P.; Gibson, V. C.; Kimberley, B. S.; Maddox, P. J.; McTavish, S. J.; Solan, G. A.; White, A. J. P.; Williams, D. J. *Chem. Commun.* **1998**, 849.
(15) Britovsek, G. J. P.; Bruce, M.; Gibson, V. C.; Kimberley, B. S.; Maddox, P. J.; Mastroianni, S.; McTavish, S. J.; Redshaw, C.; Solan, G. A.; Strömberg, S.; White, A. J. P.; Williams, D. J. *J. Am. Chem. Soc.* **1999**, *121*, 8728.
(16) Dias, E. L.; Brookhart, M.; White, P. S. *Organometallics* **2000**, *19*, 4995.
(17) Cetinkaya, B.; Cetinkaya, E.; Brookhart, M.; White, P. S. *J. Mol. Catal., A* **1999**, *142*, 101.
(18) Haarman, H. F.; Ernsting, A. L.; Kranenburg, M.; Kooijman, H.; Veldman, N.; Spek, A. L.; Elsevier, C. J.; van Leeuwen, P. W. N. M.; Vrieze, K. *Organometallics* **1997**, *16*, 887.
(19) Haarman, H. F.; Bregman, F. R.; van Leeuwen, P. W. N. M.; Vrieze, K. *Organometallics* **1997**, *16*, 979.
(20) Haarman, H. F.; Kaagman, J.-W.; Smeets, W. J. J.; Spek, A. L.; Vrieze, K. *Inorg. Chim. Acta* **1998**, *270*, 34.
(21) Kooijman, H.; Kaagman, J. W.; Mach, K.; Spek, A. L.; Schreurs, A. M. M.; Haarman, H. F.; Vrieze, K.; Elsevier, C. J. *Acta Crystallogr., Sect. C* **1999**, *C55*, 1052.
(22) Small, B. L.; Brookhart, M.; Bennett, A. M. A. *J. Am. Chem. Soc.* **1998**, *120*, 4049.
(23) Small, B. L.; Brookhart, M. *Macromolecules* **1999**, *32*, 2120.
(24) Cremer, C.; Jacobsen, H.; Burger, P. *Chimia* **1997**, *51*, 650.

10.1021/om010185y CCC: $20.00
Publication on Web 09/11/2001

Scheme 1

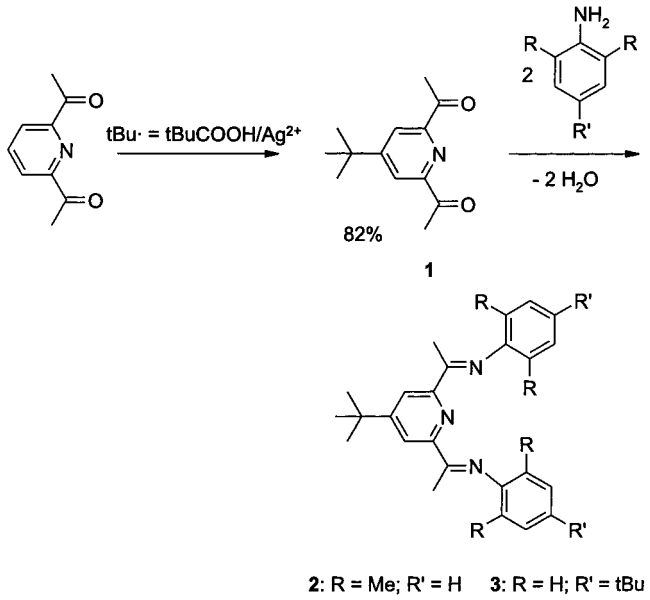

Results and Discussion

Ligands. The class of pyridine−diimine ligands used herein was introduced by Aleya et al.[11] and its chemistry more recently extended by several groups.[12−23] Due to solubility restrictions, dichloromethane solvent is most commonly used in these systems. This is of particular interest, since Vrieze et al. showed that, in addition to more common electrophiles, oxidative addition of dichloromethane also proceeds rather easily in sq-pl rhodium(I) systems bearing this ligand system to give chloromethyl Rh(III) (Rh−CH_2Cl) complexes.[18,20] To avoid this solvent, a modified version of the ligand system was sought to increase the solubility in less polar/reactive solvents: e.g., benzene. Therefore, we introduced a *tert*-butyl group into the peripheral 4-position of the pyridine ring through radical nucleophilic substitution in 2,6-diacetylpyridine with t-Bu• radicals using Minisci conditions (Scheme 1).[25] From this reaction the novel pyridine derivative **1** could be isolated in 82% yield (Scheme 1). Further conversion of **1** to the novel pyridine−diimine ligands **2** and **3** was achieved from **1** and 2,6-dimethylaniline and 4-*tert*-butylaniline, respectively, using standard conditions as described in the literature for the unsubstituted pyridine derivatives (Scheme 1).[11,15,19,22]

Complexes. Initially, the rhodium(I) and iridium(I) chloro complexes **4**−**9** were sought as starting materials for the synthesis of their corresponding Rh,Ir(I) alkyl and hydride compounds. In analogy to the syntheses by Vrieze et al.,[18] complexes **4**−**6** were obtained according to Scheme 2 from the bis(μ-chloro) dimer [Rh(C_2H_4)$_2$-Cl]$_2$, in excellent yields. It should be noted that the synthesis of complex **5** was independently reported by Brookhart et al.,[16] while we were in the last stage of composing our paper.

Complexes **4** and **5** are sparingly soluble in aromatic solvents and diethyl ether and dissolve well in THF and dichloromethane. As anticipated, the incorporation of the *tert*-butyl substituent into the pyridine ring of complex **6** significantly increases its solubility in solvents of low polarity so that benzene or toluene can be used for further transformations.

Scheme 2

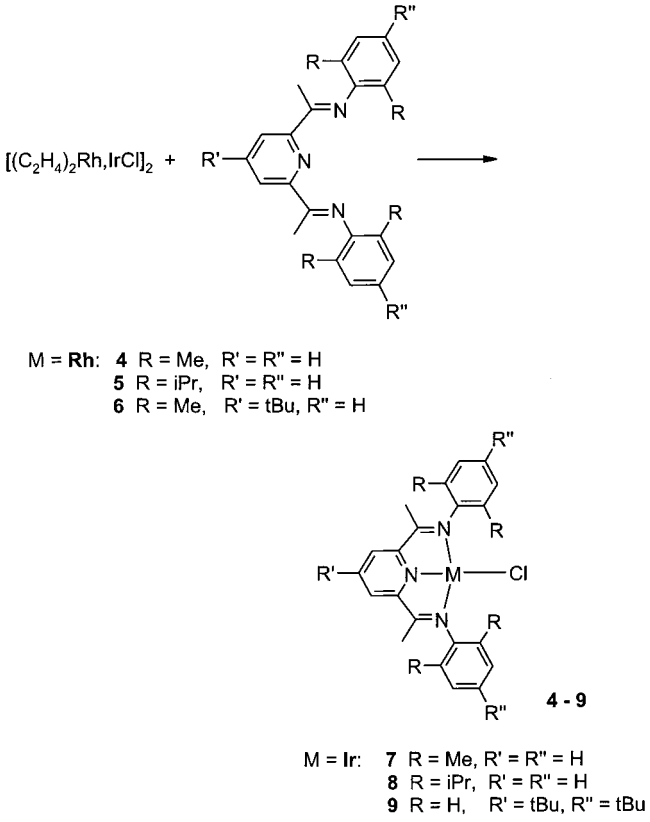

Following a synthetic procedure by Crabtree et al. for Ir compounds,[26] we obtained the analogous novel Ir complexes **7**−**9** from the reaction of the free ligands and [(C_2H_4)$_2$IrCl]$_2$ (Scheme 2). Although **7**−**9** can also be obtained from [(C_2H_4)$_2$IrCl]$_2$ prepared in situ (from ethylene and [(cyclooctene)$_2$IrCl]$_2$), compounds **7**−**9** are prepared preferably from the isolated Ir starting material (cf. the Experimental Section).

The Rh and Ir chloro complexes **4**−**9** were obtained in moderate to excellent yields as dark green (Rh) or brown (Ir) analytically pure compounds. The structural assignment was initially based on ^{1}H and ^{13}C NMR spectroscopic data, which provided support for a square-planar C_{2v}-symmetrical ligand environment. This was unambiguously confirmed by an X-ray crystal structure analysis of the rhodium compound **4**, presented in Figure 1. Details of the data collection are compiled in Table 1.

The square-planar coordination mode in complex **4** was clearly evidenced through the sum of angles of 360.0° around the Rh center. The Rh−Cl unit (Rh1−Cl1 = 2.3250(6) Å) leaves a small coordination gap for the aryl substituents of the imine moieties and thus apparently enforces a torsional angle (averaged) of 79.7° between these groups.

In analogy to the aforementioned results by Vrieze et al.,[19] both the Rh and Ir compounds react quickly and quantitatively with O_2 to give the corresponding peroxide adducts. Details of the chemistry of the Rh(III)

(25) Fontana, F.; Minisci, F.; Barbosa, M. C. N.; Vismara, E. *Tetrahedron* **1990**, *46*, 2525.

(26) Tanke, R. S.; Crabtree, R. H. *Inorg. Chem.* **1989**, *28*, 3444.

Table 1. Crystal and Data Collection Parameters for Compounds 4, 11, 13, 18, 19, and 21

	4·THF	**11**·$2CH_2Cl_2$	**13**·$2CH_2Cl_2$	18	19	**21**·(toluene)
formula	$C_{29}H_{30}ClN_3ORh$	$C_{33}H_{42}Cl_5F_3N_3O_3RhS$	$C_{30}H_{34}Cl_4F_6N_3O_6RhS_2$	$C_{29}H_{32}F_6N_3O_6RhS_2$	$C_{25}H_{31}BN_3Rh$	$C_{33}H_{38}N_3OIr$
fw	574.9	897.9	955.4	799.6	487.3	684.9
habitus	green cube	brown rect parallelepiped	orange rect parallelepiped	orange rect parallelepiped	green rect parallelepiped	green
cryst size (mm)	0.2 × 0.2 × 0.2	0.2 × 0.2 × 0.3	0.1 × 0.15 × 0.25	0.2 × 0.2 × 0.3	0.15 × 0.40 × 0.50	0.1 × 0.2 × 0.25
cryst syst	monoclinic	monoclinic	monoclinic	monoclinic	orthorhombic	orthorhombic
space group	$P2_1/n$ (No. 14)	$P2_1/n$ (No. 14)	$P2_1/c$ (No. 14)	$P2_1/n$ (No. 14)	$P2_12_12_1$ (No. 19)	*Pbca* (No. 61)
a (Å)	9.778(1)	16.173(1)	21.188(2)	12.789(1)	12.897(1)	7.891(1)
b (Å)	10.731(1)	11.947(1)	8.592(1)	17.025(1)	12.919(1)	21.861(2)
c (Å)	26.763(2)	21.088(1)	21.242(2)	15.886(1)	14.349(1)	34.144(2)
β (deg)	95.71(1)	109.81(1)	91.21(1)	110.91(3)		
V (Å^3)	2794.2(4)	3833.5(4)	3865.9(7)	3231.1(4)	2390.8(3)	5890.2(8)
Z	4	4	4	4	4	8
calcd density (g/cm^3)	1.37	1.56	1.64	1.64	1.35	1.545
temp (K)	183	183	183	183	123	183
λ(Mo Kα) (Å)	0.710 73	0.710 73	0.710 73	0.710 73	0.710 73	0.710 73
scan type	image plate	image plate	image plate	image plate	image plate	image plate
2θ range (deg)	4−48	4−48	4−48	4−52	5−53	4−45
no. of rflns measd: total, unique	17 922, 4204	12 914, 5815	24 059, 5604	24 576, 6168	15 427, 4584	14 823, 3625
no. of params	322	452	516	431	293	351
R1($F^2 > 2\sigma(F^2)$)	0.0233	0.0573	0.0441	0.0190	0.0210	0.0313
wR2($F^2 > 2\sigma(F^2)$)	0.0640	0.1577	0.1295	0.0387	0.0425	0.085
GOF, *S*	1.023	1.003	1.005	1.004	1.025	1.004
residual electron density (e/Å^3)	0.54, −0.45	0.85, −1.29	0.52, −0.59	0.34, −0.38	0.43, −0.30	1.059, −0.659

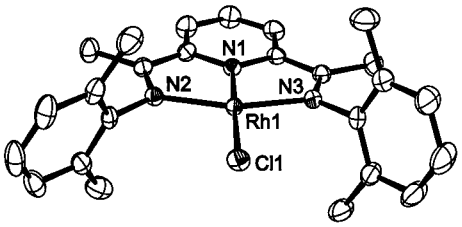

Figure 1. Ortep plot of the rhodium chloro complex **4** shown at the 50% probability level. A molecule of cocrystallized THF has been omitted for clarity. Selected bond distances (Å) and angles (deg): Rh1−Cl1 = 2.3250(6), Rh1−N1 = 1.8899(19), Rh1−N2 = 2.0348(17), Rh1−N3 = 2.0286(18); Cl1−Rh1−N1 = 178.98(5), Cl1−Rh1−N2 = 101.66(5); Cl1−Rh1−N3 = 99.83(6), N1−Rh1−N2 = 79.25(7), N1−Rh1−N3 = 79.25(8), N2−Rh1−N3 = 158.46(8).

and Ir(III) peroxide complexes and the X-ray crystal structures of **8** and its peroxide adduct will be published in a separate communication in due course.

In a next step, we intended to convert complexes **4** and **7** to the corresponding methyl compounds. However, even using a wide variety of alkylating reagents, such as MeMgCl, $AlMe_3$, $SnMe_4$, LiMe, *n*-Bu_2Mg, and Li_2CuMe_2, either just unreacted starting material was recovered ($AlMe_3$, $SnMe_4$) or complicated, intractable mixtures of products were obtained. Since the ^{1}H NMR spectra of the major component in these mixtures evidenced a symmetry lower than C_{2v}, this provided some evidence that nucleophilic attack (deprotonation) occurred also at the ketimine group, which therefore interfered with chloride substitution at the metal center. This was further substantiated through the following experiment: when complex **4** was stirred with NaOMe in methanol-d_4, in addition to metathesis of the chloride ligand with the methoxide group (vide infra), complete H/D exchange in the imine methyl groups to give −C(CD$_3$)=N(aryl) was observed.

Since attempts to obtain Rh,Ir(I) hydride complexes from the reaction of the corresponding chloro complexes **4** and **7** with hydride transfer reagents, e.g. $LiAlH_4$, $NaBH_4$, and Red-Al, were also unsuccessful, a better leaving group, e.g. a triflate ligand (OTf), was sought to facilitate the substitution at the metal center. Therefore, metathesis of the chloride groups in compounds **4** and **5** with 1 equiv of AgOTf was attempted. However, this was thwarted by the fact that a competing reaction leading to the corresponding oxidized Rh,Ir(III) complexes and elemental silver occurred. This could be confirmed by comparison of the ^{1}H NMR spectrum of the Rh(III) tris(triflate) product obtained from the reaction of **4** with 3 equiv of AgOTf in dimethoxyethane. Alternative routes to the triflate-substituted starting materials such as the conversion of the chloro complexes with (trimethylsilyl)triflate (Me_3SiOTf) and trifluoromethanesulfonic acid (HOTf) were therefore attempted. However, rather expectedly (cf. below), these reactions led to the corresponding Rh,Ir(III) oxidative addition products. In the reaction of the chloro complexes **4** and **7** with HOTf, for instance, we obtained in excellent yields the pseudo-octahedral hydrido chloro triflate Rh,Ir(III) complexes **10** and **12** with the chloro ligand in the equatorial plane and the hydride and OTf ligands in the (trans) axial positions (Scheme 3).[27] An alternative access to the Rh,Ir(I) alkyl complexes was therefore sought by reduction of the corresponding Rh(III),Ir(III) alkyl compounds. Since Vrieze et al. had previously shown that oxidative addition of dichloromethane and benzyl chloride to diimine−pyridine Rh(I) metal centers is facile,[18] we anticipated a similar reactivity of compounds **4**−**9** toward methyl triflate, MeOTf. Indeed, the desired bis(triflate) Rh,Ir(III) methyl complexes **13**−**15** were obtained in excellent yields from the reaction of Rh,Ir(I) compounds with excess (5−6 equiv) MeOTf (Scheme 3).[28]

(27) The structural assignment is based on an X-ray crystal structure of compound **10**. Crystal data: orthorhombic crystal system, space group $P2_12_12_1$ (No. 19), *a* = 12.997(1) Å, *b* = 14.833(2) Å, 19.596(1) Å. Nückel, S.; Burger, P. Unpublished results.

Scheme 3

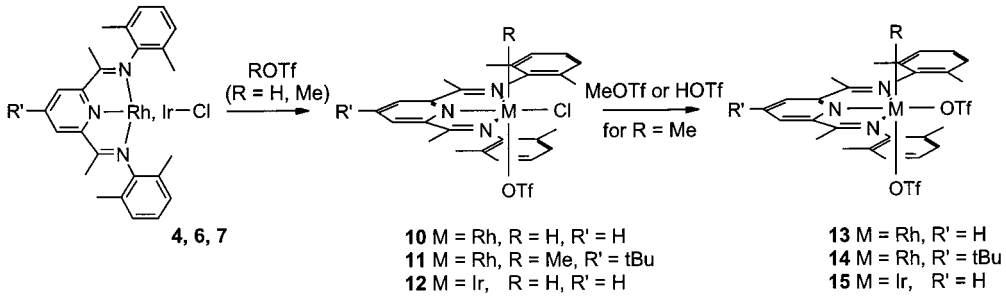

It is noteworthy that the corresponding chloro triflate complexes were obtained when these reactions were carried out with the stoichiometric amount of MeOTf. For both the rhodium chloro triflate compound **11** and the rhodium bis(triflate) complex **13**, we performed X-ray crystal structure analyses (Figures 2 and 3). The details of the data collection and refinement are tabulated in Table 1.

The geometric parameters around the Rh center in the X-ray crystal structures of complexes **11** and **13** are quite similar and clearly evidence the anticipated pseudo-octahedral ligand environment. The trans position of the methyl and triflate groups in the chloro triflate compound **11** is consistent with the generally accepted mechanism[29] for the reaction of sq-pl d^8 transition-metal complexes with polar electrophiles; i.e., nucleophilic attack of the metal center at the electrophile is followed by recombination of the cationic metal complex and the triflate anion. It deserves special mention that the methyl group in the pseudo-octahedral complexes exhibits a pronounced trans influence, which is best seen by comparison of the Rh−O distances of 2.093(3) Å (Rh1−O1) for the equatorial (cis) and 2.305(4) Å for the axial (trans) triflate groups (Rh1−O4) in **13**. On the basis of a comparison with distances observed in the X-ray crystal structures of related Rh(III) and Ir(III) triflate complexes,[24,30−35] covalent bonding of the equatorial triflate ligand is deemed, while the bond to the axial OTf group is suggested to have a pronounced ionic character. This is supported by the IR spectrum of **13** in CD_2Cl_2, which displays two bands at 1328 and 1293 cm^{-1} in the expected range for covalent and ionic triflate groups.[36,37] Furthermore, we have carried out molar conductivity measurements in CH_2Cl_2. Although the latter study clearly showed that the OTf ligand in complex **13** is not fully dissociated in this solvent, i.e., *not a* 1:1 electrolyte, concentration-dependent measurements in the range of 10^{-3} to 5×10^{-6} M provided clear evidence for a weakly dissociated ionophore (10^{-3} M, $\Lambda_M = 1.3$ S cm^{-2} mol^{-1}; 5×10^{-6} M, $\Lambda_M = 20$ S cm^{-2} mol^{-1}). Finally, the ^{19}F NMR spectrum of **13** in CD_2Cl_2, which displays resonances for two inequivalent OTf groups with a 1:1 integration ratio at δ −81.6 and −80.76 ppm, respectively, is also noteworthy.

The electronic properties of the metal methyl unit in complexes **11** and **13**−**15** deserve a special mention. From the fact that the rhodium- and iridium(III) methyl compounds are recovered quantitatively when reacted with even a large excess of HOTf, it can be readily seen that the metal-attached methyl groups display a low nucleophilicity. This is also emphasized by the fact that the methyl chloro compound **11** can be converted to the bis(triflate) complex **14** by reaction with excess (3 equiv) HOTf. This is in contrast with the chemistry of the related $Cp^*Ir(PMe_3)Me_2$[33] and $CnRhMe_3$ (Cn = trimethylazacyclonane)[38] complexes, which undergo fast reactions with 1 or 2 equiv of HOTf to give the corresponding mono- and bis(triflate) complexes. Therefore, we wish to attribute an *electrophilic* character to the methyl group in these rhodium(III) compounds, i.e., $[Rh]-Me^{\delta+}$, which would parallel the findings of Bercaw et al. in related aquo chloro d^6-Pt(IV) alkyl complexes.[39]

In a next step, we attempted to prepare the desired Rh(I),Ir(I) methyl compounds by reduction of the Rh(III) and Ir(III) complexes **13** and **15** with either $(Me_2N)_2C{=}C(NMe_2)_2$ or cobaltocene (Cp_2Co) in dimethoxyethane (dme). However, rather than the expected sq-pl d^8-configured methyl compounds, in a very clean reaction we obtained the corresponding Rh(I) and Ir(I) triflate complexes and ethane (Scheme 4). The formation of the rhodium triflate complex **16** was unambiguously established by comparison with the spectroscopic data of the independently prepared compound (see below), while the exclusive formation of ethane was confirmed by ^1H NMR spectroscopy and GC/MS spectrometry. Although the desired Ir,Rh(I) methyl complexes could thus not be obtained by reduction, the observed C−C coupling process has prompted us to investigate this reaction in more detail. As will be detailed in a separate publication in due course, the proposed mechanism involves reductive elimination of ethane from a dimethyl mono(triflate) intermediate, i.e., $(N_3)RhMe_2^+OTf^-$ (not shown; N_3 = terdentate N,N,N ligand), which is formed from **13** and the initially formed corresponding Rh(I) methyl compound **22**. The proposed mechanism is supported by the reaction of the Rh(I) methyl compound **22** with the methyl bis(triflate) complex **13**, which leads to the Rh(I)

(28) After this part of this study, a closely related complex was very recently reported by Brookhart et al. in ref 16.

(29) Collman, J. P.; Hegedus, L. S.; Norton, J. R.; Finke, R. G. *Principles and Applications of Organotransition Metal Chemistry*, 2nd ed.; University Science Books: Mill Valley, CA, 1987.

(30) Woerpel, K. A.; Bergman, R. G. *J. Am. Chem. Soc.* **1993**, *115*, 7888.

(31) Schnabel, R. C.; Roddick, D. M. *Organometallics* **1996**, *15*, 3550.

(32) Jiménez, M. V.; Sola, E.; Martínez, A. P.; Lahoz, F. J.; Oro, L. A. *Organometallics* **1999**, *18*, 1125.

(33) Burger, P.; Bergman, R. G. *J. Am. Chem. Soc.* **1993**, *115*, 10462.

(34) Bosch, M.; Laubender, M.; Weberndorfer, B.; Werner, H. *Chem. Eur. J.* **1999**, *5*, 2203.

(35) Bleeke, J. R.; Behm, R. *J. Am. Chem. Soc.* **1997**, *119*, 8503.

(36) Lawrance, G. A. *Chem. Rev.* **1986**, *86*, 17.

(37) Stang, P. J.; Huang, Y.-H.; Arif, A. M. *Organometallics* **1992**, *11*, 231.

(38) Wang, L.; Flood, T. C. *J. Am. Chem. Soc.* **1992**, *114*, 3169−3179.

(39) Luinstra, G. A.; Labinger, J. A.; Bercaw, J. E. *J. Am. Chem. Soc.* **1993**, *115*, 3004.

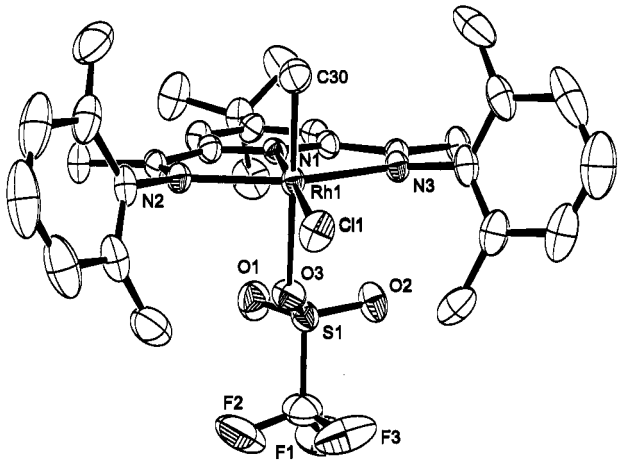

Figure 2. Ortep plot of the Rh(III) methyl chloro triflate complex **11** shown at the 50% probability level. Two molecules of cocrystallized dichloromethane have been omitted for clarity. Selected bond distances (Å) and angles (deg): Rh1−Cl1 = 2.3532(16), Rh1−N1 = 1.916(5), Rh1−N2 = 2.073(5), Rh1−N3 = 2.075(5), Rh1−O3 = 2.388(4), Rh1−C30 = 2.029(6); Cl1−Rh1−N1 = 176.25(14); Cl1−Rh1−N2 = 100.50(14); Cl1−Rh1−N3 = 101.15(14), Cl1−Rh1−O3 = 95.09(12), Cl1−Rh1−C30 = 88.0(2), N1−Rh1−N2 = 79.32(19), N1−Rh1−N3 = 79.18(19), N1−Rh1−O3 = 81.17(18), N1−Rh1−C30 = 95.7(2), N2−Rh1−N3 = 158.30(19), N2−Rh1−O3 = 89.83(17), N2−Rh1−O3 = 89.6(2), N3−Rh1−O3 = 89.74(17), N3−Rh1−C30 = 89.6(2), O3−Rh1−N3 = 176.9(2).

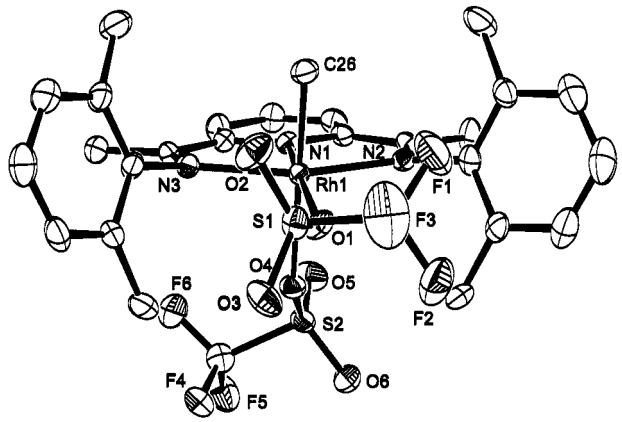

Figure 3. Ortep plot (50% probability level) of the Rh(III) methyl bis(triflate) complex **13**. Two molecules of cocrystallized dichloromethane have been omitted for clarity. Selected bond distances (Å) and angles (deg): Rh1−N1 = 1.917(4), Rh1−N2 = 2.073(4), Rh1−N3 = 2.085(4), Rh1−O1 = 2.093(3), Rh1−O4 = 2.305(4), Rh1−C26 = 2.015(5); N1−Rh1−N2 = 79.32(16), N1−Rh1−N3 = 80.16(16), N2−Rh1−N3 = 158.84(16), N1−Rh1−O1 = 172.20(16), N1−Rh1−O4 = 86.85(15), N1−Rh1−C26 = 95.3(2), N2−Rh1−O1 = 97.87(15), N2−Rh1−O4 = 93.80(15), N2−Rh1−C26 = 87.24(19), N3−Rh1−O1 = 103.14(14), N3−Rh1−O4 = 90.18(14), N3−Rh1−C26 = 89.58(19), O1−Rh1−O4 = 86.07(14), O1−Rh1−C26 = 91.76(18), O4−Rh1−C26 = 177.71(17).

triflate complex **16** and ethane within a few seconds at room temperature.

Although the yields of the triflate complex **16** obtained by reduction of **13** were quite reasonable, we attempted to find a more convenient approach to prepare this starting material. In a first step, we synthesized the novel ethylene complex **17**, from the bis(ethylene) Rh(I) triflate starting material $[Rh(C_2H_4)_2(THF)_nOTf]$, in analogy to a route described by Taube et al. for the synthesis of a related rhodium complex with a P,N,P pincer ligand (Scheme 5).[40] Complex **17** was obtained according to Scheme 5 in excellent yield as an analytically pure, microcrystalline green compound. The NMR spectroscopic data and the limited results of a strongly disordered X-ray crystal structure of **17** clearly evidenced a square-planar ligand environment with an ionic, noncoordinated triflate group. Although a comparison of the ^{1}H NMR and the ^{13}C NMR chemical shifts (^{1}H NMR, 3.39 ppm; ^{13}C NMR, 78.7 ppm) of the C_2H_4 ligand with the chemical shifts of free ethylene suggested sizable back-donation to the coordinated ethylene, this was questioned by the essentially unchanged $^1J_{C-H}(C_2H_4)$ coupling constant of 158 Hz in **17**. Therefore, it was sought that ethylene could be thermally deliberated from the ethylene complex. In a nearly quantitative reaction, this could be indeed be achieved upon heating **17** to 100 °C in dimethoxyethane (dme) using a dynamic vacuum for several days (Scheme 5).

Scheme 4

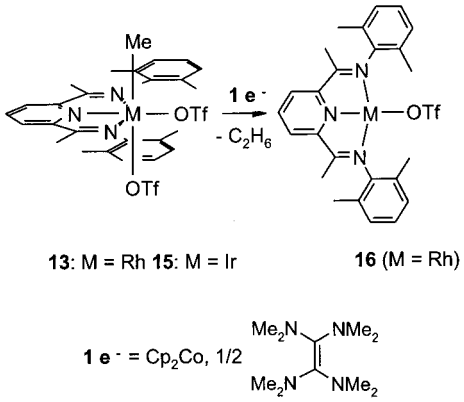

This reaction led to a green-brownish product, which was analyzed correctly as **16**·dme. At present, we do not have X-ray diffraction data for **16**·dme, so that the structural assignment is based mostly on the IR and NMR spectroscopic data. The IR spectrum of **16** displays a band at 1317 cm^{-1}, which is in the typical range of a covalent triflate group.[37] However, since the corresponding chloro complex **4** displays a band at the same position, the latter cannot be unambiguously assigned to a vibration of the triflate ligand. The ^{1}H NMR chemical shifts of a dme sample and the dme protons in **16**·dme display identical chemical shifts in CD_2Cl_2, with no detectable homonuclear NOEs between the protons of **16** and those of dme. These data thus provide evidence for a covalently bound triflate group in **16**. This was also supported through concentration-dependent molar conductivity measurements in CH_2Cl_2. Nevertheless, the latter evidenced substantial ionization of the triflate ligand through molar conductivities of $\Lambda_M = 12$ S cm^{-2} mol^{-1} and $\Lambda_M = 50$ S cm^{-2} mol^{-1} at 10^{-3} and 10^{-5} M, respectively. Support for the ionization of the triflate ligand in **16** was provided also by the X-ray crystal structure of **16**·THF, which was obtained in the course of the study of the C−C coupling process shown in Scheme 4. The molecular structure of the latter complex clearly evidenced an ionic triflate ligand with

(40) Hahn, C.; Sieler, J.; Taube, R. *Chem. Ber./Recl.* **1997**, *130*, 939.

Scheme 5

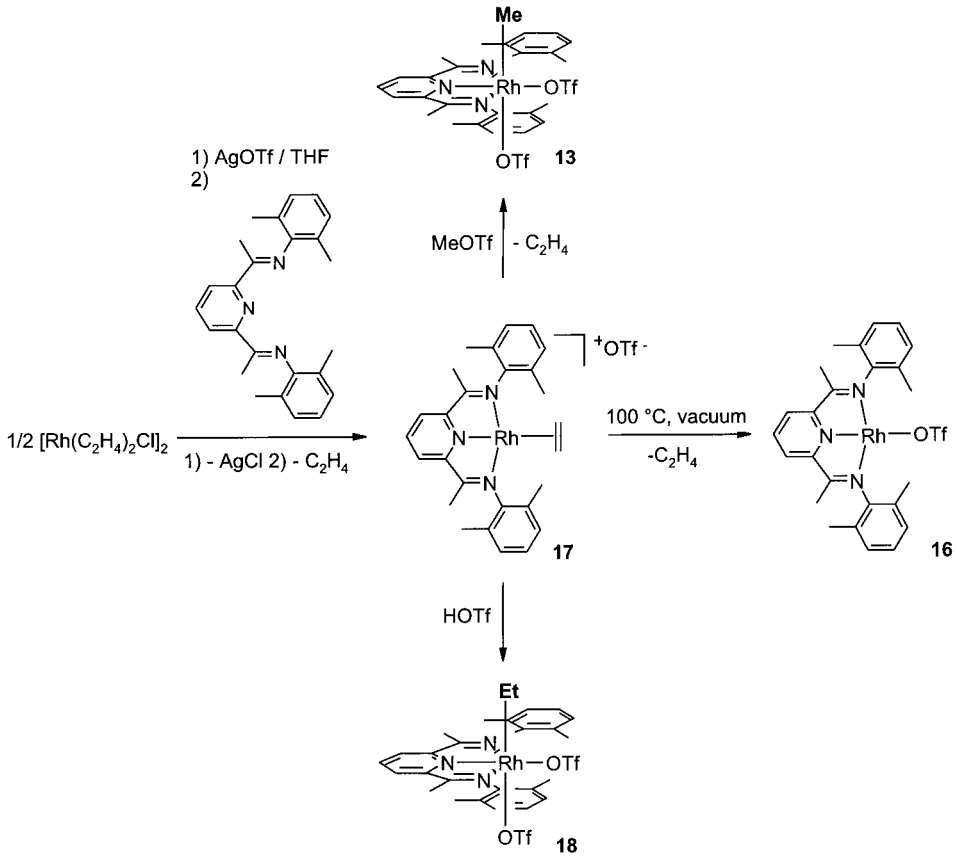

the THF ligand coordinated to the Rh center to give a sq-pl cationic Rh(I) fragment.[41] Finally, it is noteworthy that a related cationic tricoordinate Rh complex was reported by Brookhart et al. while this paper was under review. [42]

The reaction of the ethylene complex **17** with HOTf is particularly noteworthy and leads to the olefin insertion product, i.e., the ethyl bis(triflate) complex **18** (Scheme 5). The latter compound was isolated as an analytically pure compound in quantitative yield and has been fully characterized by ^{1}H and ^{13}C NMR spectroscopy and additionally by X-ray crystallography (Figure 4). The details of data collection and refinement are tabulated in Table 1.

This is in contrast with the reaction of the olefin complex **17** with MeOTf, which leads in excellent yields to the Rh(III) oxidative addition product **13** and free ethylene (Scheme 5). It deserves a special mention that we could not detect the resonances of an intermediate, e.g. the Rh(III) ethylene methyl triflate complex, while monitoring the reaction by ^{1}H NMR spectroscopy. It should be noted, however, that a closely related rhodium ethylene methyl complex was obtained by a different route in the aforementioned very recent publication of Brookhart et al.[16]

In comparison with the reaction of the ethylene complex **17** with HOTf, this implies a higher barrier for the insertion of the olefin into the rhodium−methyl bond to give the corresponding propyl triflate complex. It should be noticed that larger activation enthalpies for migratory insertion into M−Me compared to a M−H bond have been previously established.[43] Considering the low nucleophilicty of the Rh−Me methyl moiety in the methyl bis(triflate) complex **13** (vide supra), we anticipate that this contributes additionally to the higher barrier for the methyl migratory process.

Furthermore, direct conversion of the Rh(I) triflate complex **16** to the corresponding methyl complex **22** with methylating reagents such as $ZnMe_2$, $SnMe_4$ (no reaction), and $AlMe_3$ was attempted. While the ^{1}H NMR spectrum of the dark green crude reaction mixture obtained from **16** and $AlMe_3$ looked quite promising, we had problems in isolating the pure methyl complex **22**, which we attributed to coordination of the aluminum species formed in this reaction to **22**. Some support for this view was provided through the BH_4^- adduct **19**, which was obtained from the reaction of **16** with $NaBH_4$ (Scheme 6). This reaction led in good yield to the η^2-coordinated BH_4 adduct **19**. It deserves special mention that **19** is not available from the chloro complex **4**, which emphasizes the importance of a good leaving group in the Rh(I) starting material. The ^{1}H NMR resonances of the BH_4 unit are rather broad and could only be located at −100 °C as a broad pseudo-doublet. The IR bands originating from the BH_4 group are located at $\nu(^{10}BH_4/^{11}BH_4)$ 2405/2363 and 1914/1901 cm^{-1}, with the assignment being confirmed by the IR spectrum of the BD_4 isotopomer (see the Experimental Section). Prior to the X-ray crystal structure analysis of **19**, the IR bands thus provided support for an η^2-coordination of the BH_4 group by comparison with the IR data of previously character-

(41) Nückel, S.; Burger, P. Manuscript in preparation.
(42) Dias, E. L.; Brookhart, M.; White, P. S. *Chem. Commun.* **2001**, 423.
(43) Tempel, D. J.; Johnson, L. K.; Huff, R. L.; White, P. S.; Brookhart, M. *J. Am. Chem. Soc.* **2000**, *122*, 6686.

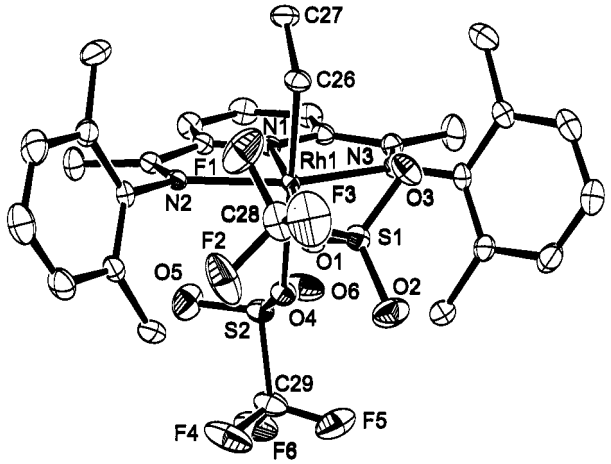

Figure 4. Ortep plot (50% probability level) of complex **18**. Selected bond distances (Å) and angles (deg): Rh1−N1 = 1.9117(14), Rh1−N2 = 2.0912(14), Rh1−N3 = 2.0731(14), Rh1−O1 = 2.1008(13), Rh1−O4 = 2.3489(13), Rh1−C26 = 2.0559(17); N1−Rh1−N2 = 79.92(6), N1−Rh1−N3 = 79.84(6), N1−Rh1−O1 = 172.26(5), N1−Rh1−O4 = 84.42(6), N1−Rh1−C26 = 95.72(7), N2−Rh1−N3 = 159.64(6), N2−Rh1−O1 = 98.26(5), N2−Rh1−O4 = 89.04(5), N2−Rh1−C26 = 90.86(7), N3−Rh1−O1 = 102.10(5), N3−Rh1−O4 = 91.22(5), N3−Rh1−C26 = 88.93(7), O1−Rh1−O4 = 88.04(5), O1−Rh1−C26 = 91.82(6), O4−Rh1−C26 = 179.81(6).

Scheme 6

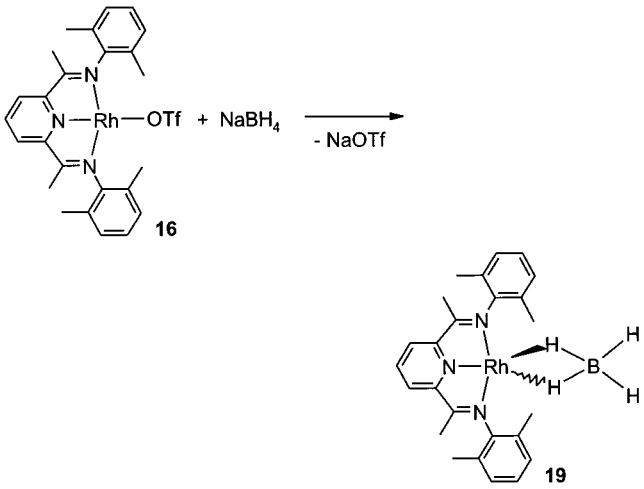

ized transition-metal BH_4 adducts.[44] This was unambiguously confirmed by X-ray crystallography (Figure 5). Data collection parameters of complex **19** are collected in Table 1.

It deserves special mention that the BH_4 adduct **19** is a rare case of a crystallographically characterized monomeric square-planar complex with a BH_4^- moiety. One of the few known compounds is the closely related terpyridine η^2-BH_4 Co(I) complex, which displays a Co−B distance of 2.162 Å.[45] Considering the larger covalent radius of rhodium, this compares well with the observed Rh1−B1 distance of 2.271(3) Å in **19**. The positions of the bridging and terminal hydrides H_b and H_t of the BH_4^- ligand could be located in the difference Fourier map and refined isotropically. From this averaged Rh1−H_b distance of 1.76(3) Å, B1−H_b = 1.24(3) Å and B1−H_t = 1.15(2) Å were derived.

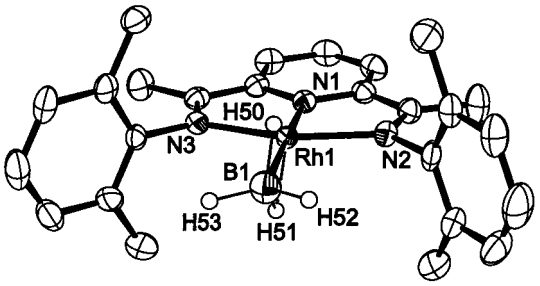

Figure 5. Ortep plot of the Rh(I) BH_4 complex **19** shown at the 50% probability level. The hydrogen atoms of the BH_4 unit have been located in the difference Fourier map and were refined isotropically. Selected bond distances (Å) and angles (deg): Rh1−N1 = 1.8939(17), Rh1−N2 = 2.0267(16), Rh1−N3 = 2.0332(16), Rh1···B1 = 2.271(3), Rh1−B1 = 2.271(3), Rh1−H50 = 1.77(2), Rh1−H51 = 1.75(3), B1−H50 = 1.26(3), B1−H51 = 1.21(3), B1−H52 = 1.15(2), B1−H53 = 1.14(2); N1−Rh1−N2 = 79.05(7), N1−Rh1−N3 = 78.72(7), N2−Rh1−N3 = 157.70(7), N1−Rh1−B1 = 178.77(9), N2−Rh1−B1 = 100.11(8), N3−Rh1−B1 = 102.15(8), N1−Rh1−H50 = 147.2(8), N1−Rh1−H51 = 147.3(9), N2−Rh1−H50 = 96.8(7), N2−Rh1−H51 = 98.1(8), N3−Rh1−H50 = 100.9(7), N3−Rh1−H51 = 101.5(8), B1−Rh1−H50 = 33.7(8), B1−Rh1−H51 = 31.8(9), H50−Rh1−H51 = 65.4(12), H50−B1−H52 = 103.9(15), H50−B1−H53 = 113.0(16), H51−B1−H52 = 114.4(17), H51−B1−H53 = 110.0(16), H52−B1−H53 = 114.2(17).

Scheme 7

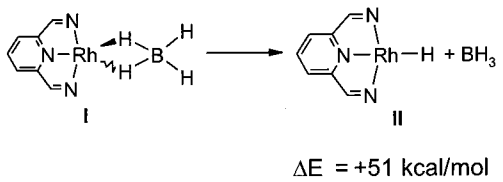

To address (a) the binding mode of the BH_4^- unit and (b) the thermodynamics for coordination of BH_3 to the Rh−H moiety, we performed DFT calculations on the unsubstituted model complexes **I** and **II** (BP-86 functional; for details see the Experimental Section).

This revealed that extrusion of BH_3 from the rhodium model complex **I** is an extraordinarily endothermic process and is uphill by 51 kcal mol^{-1} (Scheme 7). This readily explains why attempts to obtain the corresponding Rh hydride complex from **19** by removal of BH_3 as the quinuclidine·BH_3 adduct, for which we calculate a bond energy of 39 kcal mol^{-1}, were unsuccessful. In addition, we carried out a Mulliken overlap population analysis for the η^2-BH_4 model complex **I**. This evidenced a direct bonding interaction between the Rh and boron centers (0.21 e), while values of 0.31 and 0.44 e were derived for the interaction of the bridging hydrides and the Rh and B centers, respectively. As expected, a larger overlap population of 0.81 e was determined for the terminal B−H bonds.

The $RhBH_4$ unit proved to be quite robust toward methanol and trifluoroacetic acid and gave unreacted **19**, while addition of HOTf led to decomposition. Therefore, we attempted to prepare the desired corresponding hydride complex from reaction of the triflate complex **16** with hydride transfer reagents, e.g. $LiBEt_3H$ and Red-Al. However, since in all cases complicated mix-

(44) Marks, T. J.; Kolb, J. R. *Chem. Rev.* **1977**, *77*, 263.
(45) Corey, E. J.; Cooper, N. J.; Canning, W. M.; Lipscomb, W. N.; Koetzle, T. F. *Inorg. Chem.* **1982**, *21*, 192.

Scheme 8

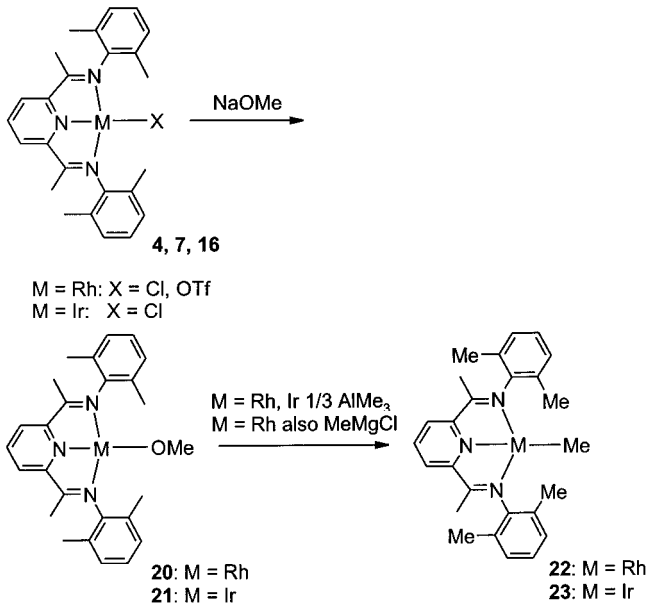

tures of products were obtained, a different starting material was sought for the syntheses of alkyl and hydride complexes. In particular, we intended to introduce a leaving group/ligand in the starting material, which (a) might provide a better driving force for ligand substitution and (b) would also help to reduce the Lewis acidity of the converted hydride/methyl transfer reagent after metathesis through π-donation, e.g. H_2BOMe.

Alkoxide complexes were thus sought as ideal starting materials. In this regard, it deserves special mention that although there are various sq-pl d^8-configured complexes bearing O−R ligands, where R = alkyl, aryl, the absolute number is still rather small.[20,21,46−55] The related aryloxide Rh complexes bearing alkyl (t-Bu and i-Pr)-substituted diimine−pyridine ligands, which have been very recently prepared by Vrieze et al. from the corresponding chloro compounds and sodium aryloxide, were therefore of particular interest.[20,21] However, since we also intended to use β-hydride elimination from the metal alkoxides as a potential route to metal hydride complexes, the methoxide-substituted compounds **20** and **21** were chosen as target molecules. The latter complexes are readily available from either the chloro and triflate complexes **4**, **7**, and **16** (Scheme 8). As has been briefly mentioned above, in addition to substitution of the chloro ligand, reaction of the rhodium and iridium chloro complexes **4** and **7** with NaOMe in deuterated methanol-d_4 led to complete H/D exchange of the

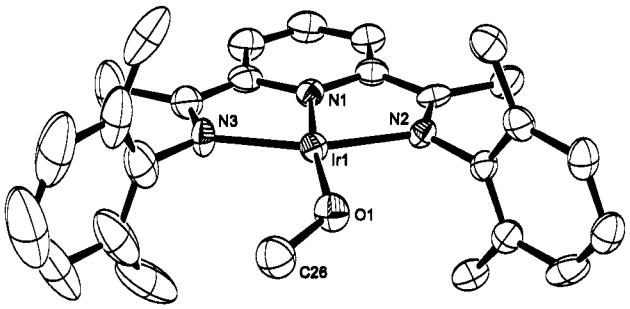

Figure 6. Ortep plot of the iridium methoxide complex **21** (50% probability level). A molecule of cocrystallized toluene has been omitted for clarity.

Table 2. Selected Distances (Å) and Angles (deg) of Compound 21

Ir1−O1	1.949(4)	Ir1−N1	1.891(5)
Ir1−N2	2.019(5)	Ir1−N3	2.012(5)
O1−C26	1.392(8)		
O1−Ir1−N1	172.63(19)	O1−Ir1−N2	93.29(18)
O1−Ir1N3	108.00(19)	N1−Ir1−N2	79.7(2)
N1−Ir1−N3	79.0(2)	N2−Ir1−N3	158.7(2)
Ir1−O1−C26	127.7(4)		
N1−Ir1−O1−C26	−153.5(13)	N3−Ir1−O1−C26	9.2(6)

Scheme 9

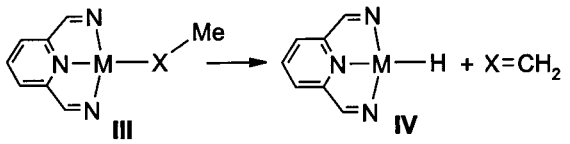

ketimine methyl groups, which was clearly evidenced through the absence of these resonances in the ^{1}H NMR spectrum and the observation of singlets at δ 1.00 and 0.42 ppm in the deuterium NMR spectrum of complexes **20-*d*$_6$** and **21-*d*$_6$** in benzene-H_6. For the Ir complex **21** we performed an X-ray crystal structure analysis, which led to the molecular structure presented in Figure 6. The data collection parameters are collected in Table 1 and selected bond distances and angles in Table 2; the structural parameters of **21** will be discussed in detail in a later section.

Complexes **20** and **21** are thermally robust, which was noticed in the attempted synthesis of the corresponding rhodium and iridium hydride complexes through β-hydrogen elimination. Upon heating complexes **20** and **21** in C_6D_6 for several days, essentially just unreacted starting material along with some minute decomposition product was observed. This is in contrast with the rather facile β-hydrogen elimination process observed by Atwood et al. and others[49−51] in sq-pl rhodium and iridium complexes in the presence of phosphine donors. Support that the reaction leading to formaldehyde and the corresponding hydride complex is thermodynamically unfavorable was provided by DFT calculations. In the latter, we also included the β-hydrogen elimination process from the rhodium ethyl model complex **III** (X = CH_2) presented in Scheme 9. A similar energetically unfavorable situation toward β-H elimination to give acetone and the [Rh]−H complex was estimated for the corresponding 2-propanolate model complex [Rh]−^{i}OPr,

(46) Bergman, R. G. *Polyhedron* **1995**, *14*, 3227.
(47) Bryndza, H. E.; Tam, W. *Chem. Rev.* **1988**, *88*, 1163.
(48) Mehrotra, R. C.; Singh, A. *Prog. Inorg. Chem.* **1997**, *46*, 239.
(49) Thompson, J. S.; Bernard, K. A.; Rappoli, B. J.; Atwood, J. D. *Organometallics* **1990**, *9*, 2727.
(50) Bernard, K. A.; Rees, W. M.; Atwood, J. D. *Organometallics* **1986**, *5*, 390.
(51) Fernandez, M. J.; Esteruelas, M. A.; Covarrubias, M.; Oro, L. A. *J. Organomet. Chem.* **1986**, *316*, 343.
(52) Miller, C. A.; Janik, T. S.; Lake, C. H.; Toomey, L. M.; Churchill, M. R.; Atwood, J. D. *Organometallics* **1994**, *13*, 5080.
(53) Kapteijn, G. M.; Dervisi, A.; Grove, D. M.; Kooijman, H.; Lakin, M. T.; Spek, A. L.; van Koten, G. *J. Am. Chem. Soc.* **1995**, *117*, 10939.
(54) Kegley, S. E.; Schaverien, C. J.; Freudenberger, J. H.; Bergman, R. G.; Nolan, S. P.; Hoff, C. D. *J. Am. Chem. Soc.* **1987**, *109*, 6563.
(55) Kuznetsov, V. F.; Yap, G. P. A.; Bensimon, C.; Alper, H. *Inorg. Chim. Acta* **1998**, *280*, 172.

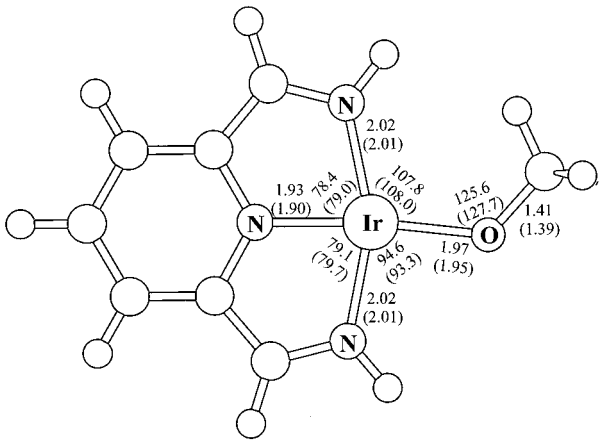

Figure 7. Selected bonding parameters of the DFT-optimized (BP-86 functional) model complex **III**, with the data observed for the X-ray crystal structure of **21** given in parentheses.

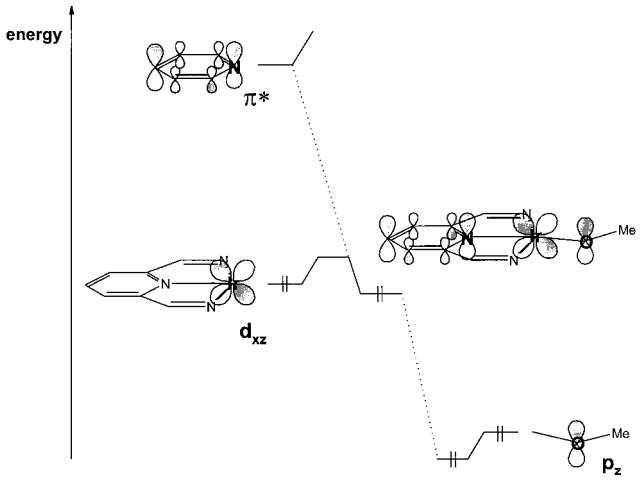

Figure 8. Fragment molecular orbital analysis (DFT, BP86) of the HOMO in the iridium methoxide model complex **III**.

for which an endothermicity of +24 kcal mol^{-1} was derived. Even though steric congestion in the 2,6-dimethylphenyl-substituted complexes **20** and **21** might favor the β-hydrogen elimination products compared to the unsubstituted model complexes, it was anticipated that the thermodynamic situation is essentially unchanged. In an exemplary fashion this was confirmed through the results of the DFT calculations on the geometrically optimized methoxide complex **20** and its hydride congener, for which an energy difference of 33 kcal mol^{-1} in favor of **20** was derived.

The reluctance of the methoxide complexes **20** and **21** to undergo β-H elimination and, in particular, the calculated strong endothermicity for the elimination of formaldehyde prompted us to study the electronic structure of the methoxide starting material in more detail. This was further stimulated by the excellent agreement of the bonding parameters of the DFT-optimized geometry of the model compound **III** (X = O, M = Ir) with the X-ray crystal structure of the Ir methoxide complex **21** (Figure 7).

The observed Ir1−O1 bond distance of 1.949(4) Å in **21** is particularly noteworthy, since to the best of our knowledge it is the shortest Ir−O bond distance observed so far for a square-planar d^8-configured Rh or Ir(I) complex bearing a monodentate alkyl- or aryloxide ligand. A comparison of the M−O distance with previously characterized compounds has to be considered with care, however, since most of the latter incorporate ligands trans to the alkoxide group, which have a significantly stronger trans influence than the pyridine group in **21**: i.e., a CO ligand or phosphine donors. Nevertheless, a particular structural feature caught our attention. This is the observed Ir−O−C bond angle of 127.7(4)° and the arrangement of the methoxide group within the plane of the Ir center and the terdentate ligand, which inferred sp^2 hybridization of the oxygen atom and, in addition, suggested π-interaction of the Ir center and the OMe group.

As has been previously discussed by Mayer et al. and others, this is in principle a four-electron−two-orbital destabilizing interaction considering the absence of an unoccupied metal-based d$_\pi$-acceptor orbital in a d^8-configured sq-pl ML$_3$X complex (X = π-donor ligand).[46,47,56] While this type of π-interaction has also been put forward by Caulton et al.,[57,58] this was recently questioned by Atwood et al. through a combined X-ray crystallographic and IR study for a series of square-planar Ir alkoxide complexes.[52] Considering these controversal results, we were interested to see whether we could establish a stabilizing interaction leading to a preference for the observed in-plane orientation of the methoxide ligand in complex **21**. This was indeed provided by the inspection of the HOMO in the model complex **III** (X = O, M = Ir), which is presented schematically in Figure 8.

The HOMO clearly displays the previously suggested π-antibonding interaction between the metal-based d$_{xz}$ and the oxygen p$_z$ orbital (notation for D_{4h} symmetry). This interaction, however, is strongly stabilized by in-phase mixing of a ligand (pyridine)-based π* acceptor orbital. To quantify this interaction, we studied the total energy dependence on the N$_{imine}$−Ir−O−C torsion angle in the methoxide model compound **III**, with the remaining geometrical parameters being fully optimized by DFT methods (BP86 functional, linear transit, Figure 9).

This evidenced a significant 11 kcal mol^{-1} preference for the in-plane coordination of the methoxide group, with the out-of-plane coordination (α = 90°) identified as a transition state (see the Experimental Section). Since a slight preference for the out-of-plane orientation of the methoxide group is deemed sterically favorable, this emphasizes the importance of the aforementioned π-back-donation to the ligand-based π* orbital, which stabilizes the otherwise four-electron−two-orbital destabilizing interaction.

Syntheses of the Rh(I) and Ir(I) Methyl Complexes 22 and 23. As anticipated, the Rh and Ir methoxy complexes **20** and **21** could be converted in excellent yields to the corresponding methyl complexes **22** and **23** through reaction with AlMe$_3$ and, for the rhodium complex **22**, also with MeMgCl (Scheme 8).

(56) Mayer, J. M. *Comments Inorg. Chem.* **1988**, *8*, 125.
(57) Lunder, D. M.; Lobkovsky, E. B.; Streib, W. E.; Caulton, K. G. *J. Am. Chem. Soc.* **1991**, *113*, 1837.
(58) Caulton, K. G. *New J. Chem.* **1994**, *18*, 25.

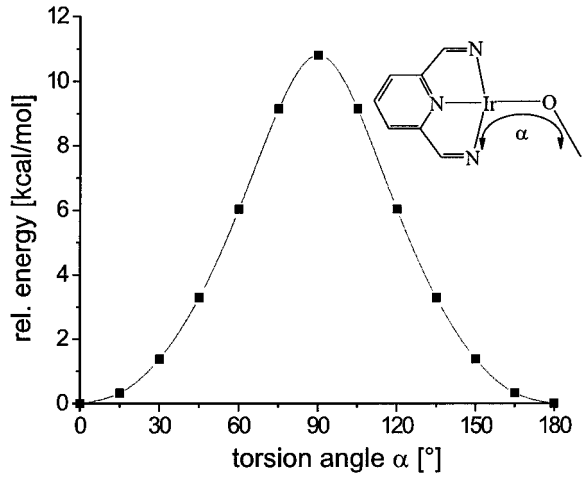

Figure 9. Walsh diagram (linear transit, DFT, BP86 functional) for the rotation about the Ir−O bond in the iridium methoxide model complex **III**.

The rhodium and iridium methyl complexes **22** and **23** were obtained as green air-sensitive analytically pure complexes, which dissolve well in aromatic solvents, e.g. benzene (for the reaction of **23** with C_6D_6 see below). The ^{1}H and ^{13}C NMR data allowed us to assign C_{2v}-symmetrical square-planar structures to **22** and **23**. The ^{1}H NMR chemical shifts of the Rh- and Ir-bound methyl groups deserve special comment. While the resonance of the Rh−Me group was in the expected range at δ 2.21 ppm, in the analogous Ir complex **23** this resonance was detected surprisingly downfield as a singlet at δ 6.91 ppm. Support for the assignment of the methyl resonance in **23** was provided by a cross-peak between this unique singlet and the ^{13}C NMR methyl resonance located at δ 2.7 ppm (assignment based on DEPT-90/135 ^{13}C NMR) in the ^{13}C−^{1}H-HSQC NMR spectrum. This assignment was unambiguously confirmed by the ^{15}N−^{1}H correlated spectrum, which displayed two cross-peaks between the Ir−Me protons and the ^{15}N resonances of the diimine and pyridine groups.

The downfield shift of the methyl resonance in **23** is likely due to the position of the methyl protons in the (downfield) anisotropic environment generated by the aryl substituents of the imine groups. This is supported by the X-ray crystal structure of the iridium complex **23**, which displays a perfect sq-pl coordination mode of the Ir center.[41] Considering that complexes of Rh and Ir are in general isostructural and display essentially identical bond angles and distances, we find the differences of the ^{1}H NMR chemical shifts of the metal-bonded methyl protons in **22** and **23** quite unusual and beyond the expected contribution of the metal center to the chemical shift. At present, we can therefore not offer an explanation for this observation; we anticipate, however, that an X-ray crystal structure of the analogous Rh complex might elucidate further details. Finally, it should be noted that we observed facile thermal *intermolecular* C−H activation of benzene in **23** to give the corresponding Ir(I) phenyl complex and methane within a few hours at room temperature. Details of this transformation, including mechanistic and theoretical studies, will be reported in due course in a separate publication.[41]

Chart 1

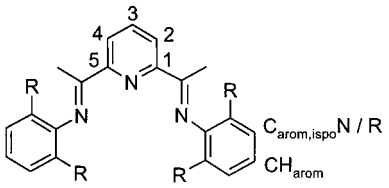

Conclusion

We have reported the syntheses of novel, reactive Rh(I) and Ir(I) triflate and methoxide complexes, which are excellent starting materials for the synthesis of Rh(I) BH_4 and Rh,Ir(I) methyl compounds. The Rh,Ir(I,III) methyl complexes described herein display very interesting reactivity patterns: i.e., C−C coupling under reactive conditions in the tervalent d^6-configured complexes and facile thermal *intermolecular* C−H activation in benzene in the Ir(I) methyl system. In due course, we will report further details of these transformations and will also elaborate on the reactions of the novel Rh(I),Ir(I) methyl complexes with H_2. In particular, we will describe the extraordinarily facile Si−H and C−H bond activation in silanes, arenes, and alkanes observed for a related diimine−pyridine Ir system.

Experimental Section

Reactions were carried out under a dinitrogen atmosphere with thoroughly dried and N_2-saturated solvents using glovebox and Schlenk techniques. 2,6-Diacetylpyridine, 2,6-dimethylaniline, 4-*tert*-butylaniline, pivalic acid, HOTf, MeOTf, $NaBH_4$, NaOMe, and $AlMe_3$ were purchased from Fluka and Aldrich and used as received. The starting materials, $[Rh(C_2H_4)_2Cl]_2$,[59] $[Rh(THF)_x(C_2H_4)_2OTf]$,[40] $[Ir(C_2H_4)_2Cl]_2$[60] and the 2,6-dimethyl-substituted (ligand **A**, *N*-(2,6-dimethylphenyl)-*N*-((1*E*)-1-{6-[(1*E*)-*N*-(2,6-dimethylphenyl)ethanimidoyl]pyridin-2-yl}ethylidene)amine) and 2,6-diisopropyl-substituted ligands (ligand **B**, *N*-(2,6-diisopropylphenyl)-*N*-((1*E*)-1-{6-[(1*E*)-*N*-(2,6-diisopropylphenyl)ethanimidoyl]pyridin-2-yl}ethylidene)-amine)[15,22] were prepared as described in the literature. ^{1}H, ^{13}C, and ^{19}F NMR spectra were recorded on Varian Mercury 200 and Gemini 300 and Bruker Avance-500 spectrometers at 298 K unless otherwise specified. Chemical shifts are given in ppm and referenced to the residual ^{1}H or ^{13}C NMR solvent shifts and for the ^{19}F NMR resonances against trifluorotoluene. The assignment of ^{1}H NMR and ^{13}C NMR resonances is based on DEPT and two-dimensional ^{1}H−^{1}H COSY, ^{13}C−^{1}H HSQC, and ^{13}C−^{1}H, ^{15}N−^{1}H HMBC experiments. The applied NMR numbering scheme shown in Chart 1 was used. IR spectra were measured on a Biorad FTS-45 Fourier IR spectrometer. X-ray crystal structure analyses were performed on a Stoe IPDS image plate system with a graphite-monochromated Mo Kα (0.707 13 Å) beam. CHN analyses were carried out with a LECO CHNS-932 elemental analyzer at our institute. GC/MS analyses were performed with a Varian Saturn 2000 GC/MS (ion trap) spectrometer with the reaction solution containing the ethane gas previously transferred/collected by standard high-vacuum manometry. Conductivity measurements were performed with an Amel-160 conductometer using glass cells with Pt electrodes (K = 0.94 and 0.11).

Synthesis of 4-*tert*-Butyl-2,6-diacetylpyridine (1). A mixture of 6.0 g (37 mmol) of 2,6-diacetylpyridine, 18.8 g (184 mmol) of pivalic acid, 1.0 g (5.9 mmol) of silver nitrate, 31.0 g

(59) Cramer, R.; McCleverty, J. A.; Bray, J. *Inorg. Synth.* **1990**, *28*, 86.

(60) Arthurs, M. A.; Bickerton, J.; Stobart, S. R.; Wang, J. *Organometallics* **1998**, *17*, 2743.

(129 mmol) of sodium peroxodisulfate ($Na_2S_2O_8$), and 5.4 g (55 mmol) of concentrated sulfuric acid was dissolved in a mixture of 350 mL of water and 60 mL of chlorobenzene and refluxed for 8 h. After the mixture was cooled to room temperature, NaOH was added until pH 9 was reached, which was followed by filtration through a sintered-glass frit. The filtrate (two-phase system) was extracted with four 10 mL portions of CH_2Cl_2. The combined organic phases were dried over Na_2SO_4, and finally the solvent was evaporated in vacuo. The oily crude product was purified by Kugelrohr distillation at 10^{-2} mbar (175 °C). Yield: colorless oil, 6.6 g (30 mmol), 82%. ^{1}H NMR ($CDCl_3$): δ 1.37 (s, 9 H, ^{t}Bu); 2.79 (s, 6 H, $-C(O)CH_3$); 8.23 (s, 2 H, CH(2,4)). $^{13}C\{^1H\}$ NMR ($CDCl_3$): δ 25.7 ($-C(O)CH_3$); 30.4 ($C(CH_3)_3$); 35.4 ($C(CH_3)_3$); 121.7 (CH (2,4)); 152.8 (C (1,5)); 162.6 (C(3)); 200.0 ($-C(O)CH_3$). Anal. Calcd for $C_{13}H_{17}NO_2$: C, 71.21; H, 7.81; N, 6.39. Found: C, 70.95; H, 7.56; N, 6.39.

Synthesis of Ligand 2. To a suspension of 2.01 g (9.2 mmol) of 4-*tert*-butyl-2,6-diacetylpyridine (**1**) and 4.44 g (36.7 mmol) of 2,6-dimethylaniline were added 6 g of molecular sieves (4 Å) in 5 mL of toluene and 5 drops of formic acid, and the mixture was stirred for 35 days. The molecular sieve was filtered off and washed with five 10 mL portions of toluene. The organic phase was concentrated under vacuum, methanol was added until a yellow precipitate was obtained, and then this mixture was placed in a refrigerator at 10 °C overnight to complete crystallization. The product was collected by filtration, washed with cold methanol, and dried in vacuo. A second crop could be obtained from the filtrate as described above. Yield: yellow crystals, 771 mg (1.73 mmol), 19% (unoptimized). ^{1}H NMR ($CDCl_3$): δ 1.16 (s, 9 H, ^{t}Bu); 2.07 (s, 12 H, CH_3); 2.25 (s, 6 H, $CN-CH_3$); 6.96−7.08 (m, 6 H, CH_{arom}); 8.85 (s, 2 H, CH(2,4)). $^{13}C\{^1H\}$ NMR ($CDCl_3$): δ 16.6 ($CN-CH_3$); 18.1 (CH_3); 30.5 ($C(CH_3)_3$); 35.1 ($C(CH_3)_3$); 119.6 (CH-(2,4)); 123.4 ($C_{arom}H$); 125.5 ($C_{arom,ipso}CH_3$); 128.4 ($C_{arom}H$); 149.5 ($C_{arom,ipso}N$); 155.8 (C(1,5)); 161.4 (C(3)); 167.3 (C=N). IR (imine range, toluene): 1644 (s, C=N), 1649 (s, C=N) cm^{-1}. Anal. Calcd for $C_{29}H_{35}N_3$: C, 81.83; H, 8.29; N, 9.88. Found: C, 81.76; H, 7.97; N, 9.93.

Synthesis of Ligand 3. A solution of 1.0 g (4.6 mmol) 4-*tert*-butyl-2,6-diacetylpyridine (**1**) and 1.7 g (11.4 mmol) 4-*tert*-butylaniline in 15 mL MeOH was treated with five drops of formic acid (98%) and stirred for 36 h at 50 °C. After 1 h the formation of a yellow solid precipitate was observed. The mixture was cooled to room temperature and the yellow solid was collected by filtration and washed with cold methanol. Recrystallization from hexane yields bright yellow crystals, which are also suitable for X-ray crystal diffraction. Yield: 407 mg (0.85 mmol) 18% (unoptimized). ^{1}H NMR (C_6D_6): δ 1.12 (s, 6 H, $CN-CH_3$); 1.25 (s, 18 H, ^{t}Bu); 2.50 (s, 9H, C(3)-^{t}Bu); 6.93 (m, 4 H, CH_{arom}); 8.82 (s, 2 H, CH(2,4)). $^{13}C\{^1H\}$ NMR (C_6D_6): δ 16.4 ($C(3)-C(CH_3)_3$); 30.4 ($CN-CH_3$); 31.6 ($C(CH_3)_3$); 34.3 ($C(CH_3)_3$); 35.3 ($C(3)-C(CH_3)_3$); 119.5 ($C_{arom}H$); 119.8 (CH(2,4)); 126.2 ($C_{arom}H$); 146.3, 149.6, 156.1, 161.1 (C(3), $C_{arom,ipso}$^{t}Bu, C(1,5), $C_{arom,ipso}N$); 167.3 (C=N). IR (imine range, toluene): 1639 (s, C=N) cm^{-1}. Anal. Calcd for $C_{33}H_{43}N_3$: C, 82.28; H, 9.00; N, 8.72. Found: C, 82.34; H, 9.12; N, 8.73.

Synthesis of the Rhodium(I) Chloro Complex 4. To a solution of 460 mg (1.18 mmol) of $[Rh(C_2H_4)_2Cl]_2$ in 20 mL of THF was slowly added 874 mg (2.37 mmol) of ligand **A** (see text above) as a solid. The resulting dark green solution was stirred for 30 min. The solvent was removed in vacuo, and the dark green solid was washed with pentane (2 × 10 mL). After drying under vacuum, the product was obtained in 99% yield (1.36 g, 2.34 mmol) as an analytically pure compound. Crystals suitable for X-ray diffraction were obtained by diffusion of pentane into a solution of **4** in THF. ^{1}H NMR (CD_2Cl_2): δ 1.61 (s, 6 H, $CN-CH_3$); 1.82 (m, 4 H, THF); 2.11 (s, 12 H, CH_3); 3.68 (m, 4 H, THF); 7.14 (s, 6 H, CH_{arom}); 7.67 (d, ^3J = 8 Hz, 2 H, CH(2,4)); 8.47 (t, ^3J = 8 Hz, 1 H, CH(3)). $^{13}C\{^1H\}$ NMR (CD_2Cl_2): δ 16.8 ($CN-CH_3$); 18.7 (CH_3); 25.9 (THF); 68.1 (THF); 124.3 (CH(3)); 125.2 (CH(2,4)); 125.9, 127.8 ($C_{arom}H$); 130.3 ($C_{arom,ipso}CH_3$); 149.0 ($C_{arom,ipso}N$); 156.6 (C(1,5)); 168.2 (C=N). MS: 507 (M^+, 10%); 471 ($M^+ - Cl$, 100%); 324 (ligand, 95%). Anal. Calcd for $C_{29}H_{35}ClN_3RhO$: C, 60.06; H, 6.08; N, 7.25. Found: C, 60.31; H, 6.15; N, 7.45. The crystalline material contains one molecule THF per complex **4**, which was confirmed by ^{1}H NMR integration.

Synthesis of the Rhodium(I) Chloro Complex 5. To a suspension of 329 mg (683 μmol) of ligand **B** (see text above) in 6 mL of THF was added dropwise a solution of 133 mg (341 μmol) of $[Rh(C_2H_4)_2Cl]_2$ in 5 mL of THF. After 5 min the slurry turned dark green. The mixture was stirred for 18 h, and then the solvents were removed under high vacuum. The resulting dark green solid is pure enough for most synthetic purposes; recrystallization from THF/pentane (1/1 v/v) at −35 °C yields **5** as an analytically pure solid. Yield: 416 mg (672 μmol), 98%. ^{1}H NMR (CD_2Cl_2): δ 1.03 (d, ^3J = 7 Hz, 12 H, $CH(CH_3)_2$); 1.13 (d, ^3J = 7 Hz, 12 H, $CH(CH_3)_2$); 1.64 (s, 6 H, $CN-CH_3$); 3.03 (sept, ^3J = 7 Hz, 4 H, $CH(CH_3)_2$); 7.30 (m, 6 H, CH_{arom}); 7.70 (d, ^3J = 8 Hz, 2 H, CH(2,4)); 8.51 (t, ^3J = 8 Hz, 1 H, CH(3)). $^{13}C\{^1H\}$ NMR (CD_2Cl_2): δ 17.8 ($CN-CH_3$); 23.58 ($CH(CH_3)_2$); 23.64 ($CH(CH_3)_2$); 28.5 ($CH(CH_3)_2$); 123.5 ($C_{arom}H$); 124.0 (CH(3)); 125.3 (CH(2,4); 126.7 ($C_{arom}H$); 140.8 ($C_{arom,ipso}$^{i}Pr); 146.1 ($C_{arom,ipso}N$); 156.5 (C(1,5)); 168.0 (C=N). MS: 619 (M^+, 100%); 583 ($M^+ - Cl$, 100%); 568 ($M^+ - Cl - CH_3$, 100%), 540 ($M^+ - Cl - {}^i$Pr, 44%). Anal. Calcd for $C_{33}H_{43}N_3ClRh$: C, 63.92; H, 6.99; N, 6.78. Found: C, 64.04; H, 6.74; N, 6.71.

Synthesis of the Rhodium(I) Chloro Complex 6. A solution of 9 mg (23 μmol) of $[Rh(C_2H_4)_2Cl]_2$ and 20 mg (46 μmol) of **2** in 5 mL of THF was stirred for 1.5 h at room temperature, giving a dark green solution. The solvent was removed in vacuo to yield a dark green solid. Recrystallization from THF/diethyl ether at −35 °C yields 27 mg (44 μmol, 98%) of **6**. ^{1}H NMR (C_6D_6): δ 1.11 (s, 6 H, $CN-CH_3$); 1.25 (s, 9 H, ^{t}Bu); 1.51 (m, $^1/_2$ THF); 2.33 (s, 12 H, CH_3); 3.68 (m, $^1/_2$ THF); 7.26 (s, 6 H, CH_{arom}); 7.42 (s, 2 H, CH(2,4)). $^{13}C\{^1H\}$ NMR (C_6D_6): δ 16.1 ($CN-CH_3$); 18.9 (CH_3); 25.5 (THF); 29.1 ($C(CH_3)_3$); 36.5 ($C(CH_3)_3$); 67.5 (THF); 120.8 (CH(2,4)); 125.8 ($C_{arom}H$); 128.2 ($C_{arom}H$); 129.9 ($C_{arom,ipso}CH_3$); 146.2 (C(3)); 149.1 ($C_{arom,ipso}N$); 156.3 (C(1,5)); 166.1 (C=N). Anal. Calcd for $C_{31}H_{39}ClN_3O_{1/2}Rh$ (contains $^1/_2$ molecule THF per molecule, confirmed by ^{1}H NMR integration): C, 62.05; H, 6.55; N, 7.00. Found: C, 62.28; H, 6.55; N, 6.78.

Synthesis of the Iridium(I) Chloro Complex 7. To a solution of 516 mg (0.91 mmol) $[Ir(C_2H_4)_2Cl]_2$ in 8 mL of toluene was added slowly a solution of 672 mg (1.82 mmol) of ligand **A** dissolved in 20 mL of toluene. First a color change to dark green was noticed, and then a brown solid precipitated. After the mixture was stirred for 30 min, the solvent was removed in vacuo. The brown solid was washed twice with 5 mL of pentane and then dried in vacuo. Unreacted free ligand was removed by washing the solid with ether (2 × 10 mL). After drying in vacuo, a brown solid is obtained; analytically pure brown (sometimes green) material is obtained by recrystallization from THF/pentane at −35 °C. Yield: 842 mg (1.41 mmol), 78%. ^{1}H NMR (CD_2Cl_2): δ 1.05 (s, 6 H, $CN-CH_3$); 2.04 (s, 12 H, CH_3); 7.19 (m, 6 H, CH_{arom}); 7.85 (d, ^3J = 8 Hz, 2 H, CH(2,4)); 8.74 (t, ^3J = 8 Hz, 1 H, CH(3)). $^{13}C\{^1H\}$ NMR (CD_2Cl_2): δ 18.7 (CH_3); 18.9 (CN-CH_3); 123.2 (CH(2,4)); 123.5 (CH(3)); 126.5, 128.1 ($C_{arom}H$); 130.8 ($C_{arom,ipso}CH_3$); 152.6 ($C_{arom,ipso}N$); 163.9 (C(1,5)); 173.4 (C=N). Anal. Calcd for $C_{25}H_{27}ClIrN_3$: C, 50.28; H, 4.56; N, 7.04. Found: C, 50.57; H, 4.63; N, 7.01.

Alternative Synthesis of the Iridium(I) Chloro Complex 7. A slow flow of ethylene was bubbled through a suspension of 408 mg (455 μmol) of $[Ir(COE)_2Cl]_2$ in 12 mL of hexane at 0 °C. After a color change from dark red to light red was noticeable, indicating the formation of $[Ir(C_2H_4)_4Cl]$, a solution of 336 mg (909 μmol) of ligand **A** in 5 mL of THF was added slowly via a drain tube, yielding a dark green (sometimes also dark brown) mixture, which was stirred for a further 10 min at 0−5 °C. After this time, the reaction mixture

was evaporated to dryness in vacuo. Recrystallization from THF/pentane at −35 °C yielded dark green crystals: 265 mg (444 μmol), 49%.

Synthesis of the Iridium(I) Chloro Complex 8. A solution of ligand **B** (141 mg, 292 μmol) dissolved in 20 mL of THF was added slowly to a solution of 83 mg (146 μmol) of $[Ir(C_2H_4)_2Cl]_2$ in 5 mL of Et_2O, and the resulting brown mixture was stirred for 3 h at room temperature. The solvents were removed under vacuum, and the remaining brown solid was washed with pentane (2 × 5 mL) and dried in vacuo. After this solid was dissolved in methanol and the solution was filtered via cannula, the green solution was evaporated to dryness in vacuo and the brown solid residue recrystallized from a mixture of THF/Et_2O, yielding 60 mg (85 μmol, 29%) of brown crystals, which dissolve in dichloromethane, toluene, or THF as a green solution. Single crystals suitable for X-ray diffraction can be obtained by the same method. ^{1}H NMR (toluene-d_8): δ 0.55 (s, 6 H, CN−CH_3); 1.02 (d, ^3J = 7 Hz, 12 H, CH(CH_3)$_2$); 1.04 (d, ^3J = 7 Hz, 12 H, CH(CH_3)$_2$); 2.97 (sept, ^3J = 7 Hz, 4 H, CH(CH$_3$)$_2$); 6.91−7.05 (m, 6 H, CH_{arom}); 7.16 (d, ^3J = 8 Hz, 2 H, CH(2,4)); 8.12 (t, ^3J = 8 Hz, 1 H, CH(3)). ^{13}C{^{1}H} NMR (toluene-d_8): δ 19.6 (CN−*C*H$_3$); 23.9 (CH(*C*H$_3$)$_2$); 24.2 (CH(*C*H$_3$)$_2$); 28.2 (*C*H(CH$_3$)$_2$); 121.6 (CH(3)); 122.3 (CH(2,4)); 123.5, 127.5 (C_{arom}H); 140.8 (*C*$_{arom,ipso}$^{i}Pr); 149.8 ($C_{arom,ipso}$N); 164.0 (C(1,5)); 171.8 (C═N). Anal. Calcd for $C_{33}H_{43}N_3ClIr$: C, 55.87; H, 6.11; N, 5.92. Found: C, 55.60; H, 6.20; N, 5.93.

Synthesis of the Iridium(I) Chloro Complex 9. A solution of 27 mg (56 μmol) of ligand **3** in 3 mL of toluene was added slowly (3 min) to a solution of 16 mg (28 μmol) of $[Ir(C_2H_4)_2Cl]_2$ in 4 mL of toluene, upon which the color changed to brown. The solvent was evaporated to dryness in vacuo, the residue redissolved in toluene, and this solution once more evaporated to dryness. The remaining dark green solid was washed twice with pentane (5 mL each) and dried in vacuo. The solid was further washed with pentane until the washing solutions were nearly colorless, yielding a bright green solid, which was dried in vacuo. Yield: 31 mg (44 μmol), 79%. ^{1}H NMR (C_6D_6): δ 0.57 (s, 6 H, CN−CH_3); 1.21 (s, 18 H, C(CH$_3$)$_3$); 1.23 (s, 9 H, C3−C(CH$_3$)$_3$); 7.36 ("d", J = 9 Hz, 4 H, CH_{arom}); 7.57 ("d", J = 9 Hz, 4 H, CH_{arom}); 7.60 (s, 2 H, CH(2,4)). ^{13}C{^{1}H} NMR (C_6D_6): δ 20.6 (CN−*C*H$_3$); 29.2 (C(3)−C(*C*H$_3$)$_3$); 31.8 (C(*C*H$_3$)$_3$); 34.9 (*C*(CH$_3$)$_3$); 37.9 (C(3)−*C*(CH$_3$)$_3$); 119.0 (CH(2,4)); 124.6, 125.7 (C_{arom}H); 146.1 (C(3)); 149.6 (*C*$_{arom,ipso}$^{t}Bu); 152.5 ($C_{arom,ipso}$N); 164.9 (C(1,5)); 171.1 (C═N). Anal. Calcd for $C_{33}H_{43}N_3ClIr$: C, 55.87; H, 6.11; N, 5.92. Found: C, 56.24; H, 6.45; N, 5.59.

Synthesis of Rh(III) Chloro Hydride Triflate Complex 10. A solution of 97 mg (167 μmol) of **4** in 5 mL of CH_2Cl_2 was reacted with 15 μL (167 μmol) of HOTf, which led to an immediate color change from dark green to bright orange. After the mixture was stirred for 30 min, the volume of the solvent was reduced to half in vacuo and then layered with pentane. Recrystallization at −35 °C yielded 104 mg (158 μmol, 95%) of orange crystals, which were also suitable for X-ray diffraction. ^{1}H NMR (CD_2Cl_2): δ −23.8 (d, ^1J(Rh,H) = 24 Hz, 1 H, Rh−H); 2.10 (s, 6 H, CH$_3$); 2.32 (s, 6 H, CH$_3$); 2.36 (s, 6 H, CN−CH$_3$); 7.08−7.18 (m, 6 H, CH_{arom}); 8.04 (d, ^3J = 8 Hz, 2 H, CH(2,4)); 8.29 (t, ^3J = 8 Hz, 1 H, CH(3)). ^{13}C NMR (CD_2Cl_2): δ 17.9 (d, ^3J(Rh,C) = 1 Hz, CN−*C*H$_3$); 18.4 (CH$_3$); 18.9 (CH$_3$); 127.5 (CH(2,4)); 127.8, 128.61, 128.63, 129.1 (C_{arom}H); 131.6 (*C*$_{arom,ipso}$CH$_3$); 139.5 (CH(3)); 144.4 ($C_{arom,ipso}$N); 158.8 (C(1,5)); 180.0 (C═N). ^{19}F NMR (CD_2Cl_2): δ −80.76 (s, OTf). ^{15}N NMR (CD_2Cl_2): δ −323.8 (pyridine); −324.5 (C═N). Anal. Calcd for $C_{26}H_{28}ClF_3N_3O_3RhS$: C, 47.46; H, 4.29; N, 6.39. Found: C, 47.37; H, 4.45, N, 6.41.

Synthesis of the Rhodium(III) Methyl Chloro Triflate Complex 11. To a solution of **6** (28 mg, 47 μmol) in 5 mL of CH_2Cl_2 was added 5 μL (47 μmol) of MeOTf, leading to a color change from green to brown. The solution was stirred for 1 h; the solvent was then reduced to half by evaporation in vacuo. Recrystallization from CH_2Cl_2/pentane yielded **11** as orange crystals, which were separated by centrifugation, washed with a small amount of diethyl ether, and finally dried under high vacuum. Yield: 25 mg (33.5 μmol), 71%. ^{1}H NMR (CD_2Cl_2): δ 1.53 (s, 3 H, Rh−C*H*$_3$); 1.54 (s, 9 H, ^{t}Bu); 2.10 (s, 6 H, CN−CH$_3$); 2.42 (s, 12 H, CH$_3$); 7.12−7.20 (m, 6 H, CH_{arom}); 8.02 (s, 2 H, CH(2,4)). ^{13}C{^{1}H} NMR (CD_2Cl_2): δ 1.3 (d, ^1J(Rh,C) = 25 Hz, Rh-*C*H$_3$); 18.9 (CH$_3$); 19.0 (CN−*C*H$_3$); 20.6 (CH$_3$); 30.5 (C(*C*H$_3$)$_3$); 36.8 (*C*(CH$_3$)$_3$); 125.6 (CH(2,4)); 127.9, 128.6, 128.8 (C_{arom}H); 129.5, 133.9 (*C*$_{arom,ipso}$CH$_3$); 144.1 ($C_{arom,ipso}$N); 158.0 (C(1,5)); 165.3 (C(3)); 180.1 (C═N). ^{19}F NMR (CD_2Cl_2): δ −80.72 (s, OTf). Anal. Calcd for $C_{31}H_{35}N_3ClF_3O_3RhS$: C, 51.35; H, 4.87; N, 5.80. Found: C, 50.99; H, 5.21; N, 5.61.

Synthesis of Ir(III) Chloro Hydride Triflate Complex 12. A 10 μL (115 μmol) portion of HOTf was added to a solution of 46 mg (77 μmol) of complex **7** in 5 mL of CH_2Cl_2 and the dark green mixture stirred for 45 min. The volume was reduced to half in vacuo and then layered with pentane. Crystallization at −35 °C yielded **12** as dark green crystals: 53 mg (71 μmol), 92%. ^{1}H NMR (CD_2Cl_2): δ −36.27 (s, 1 H, Ir−H); 1.97 (s, 6 H, CH$_3$); 2.30 (s, 6 H, CH$_3$); 2.68 (s, 6 H, CN−CH$_3$); 7.10−7.19 (m, 6 H, CH_{arom}); 7.91 (s, 3 H, CH(2,4) and CH(3)). ^{13}C NMR (CD_2Cl_2): δ 17.1 (CN−*C*H$_3$); 17.4 (CH$_3$); 18.7 (CH$_3$); 126.4 (CH(2,4) or CH(3)); 127.8, 128.7, 128.8, 129.0 (C_{arom}H); 132.0 (*C*$_{arom,ipso}$CH$_3$); 137.7 (CH(2,4) or CH(3)); 145.2 ($C_{arom,ipso}$N); 162.6 (C(1,5)); 183.4 (C═N). ^{19}F NMR (CD_2Cl_2): δ −80.71 (s, OTf). Anal. Calcd for $C_{26}H_{28}ClF_3IrN_3O_3S$: C, 41.79; H, 3.78; N, 5.62. Found: C, 41.79; H, 3.78; N, 5.45.

Synthesis of the Rhodium(III) Methyl Bis(triflate) Complex 13. A 0.36 mL (3.28 mmol) portion of methyl triflate was added to a vigorously stirred solution of 380 mg (656 μmol) of complex **4** in 30 mL of CH_2Cl_2, yielding an orange solution. From time to time MeCl was removed by applying a weak vacuum. After 4 h, the volume of the solvent was reduced under vacuum to ca. 5 mL, upon which the product precipitated as a microcrystalline orange solid. The solvent was decanted off, and the solid was washed with three 5 mL portions of ether and then dried under high vacuum. Analytically pure complex **13** was obtained by recrystallization from a mixture of dichloromethane and pentane at −35 °C. Yield: yellow solid, 433 mg (551 μmol), 84%. Single crystals suitable for X-ray diffraction were obtained upon cooling a pentane-layered dichloromethane solution to −35 °C. ^{1}H NMR (CD_2Cl_2): δ 1.91 (d, ^2J(Rh,H) = 2 Hz, 3 H, Rh−C*H*$_3$); 2.13 (s, 6 H, CH$_3$); 2.44 (s, 6 H, CH$_3$); 2.47 (s, 6 H, CN−CH$_3$); 7.12−7.21 (m, 6 H, CH_{arom}); 8.07 (d, ^3J = 8 Hz, 2 H, CH(2,4)); 8.37 (t, ^3J = 8 Hz, 1 H, CH(3)). ^{13}C{^{1}H} NMR (CD_2Cl_2): δ 4.7 (d, ^1J(Rh,C) = 24.5 Hz, Rh−*C*H$_3$); 19.0 (CN−*C*H$_3$), 19.1 (CH$_3$), 20.0 (CH$_3$), 128.4 (CH(2,4)); 128.5, 128.9, 129.0, 130.5 (C_{arom}H); 133.8 (*C*$_{arom,ipso}$CH$_3$); 140.4 (CH(3)); 143.4 ($C_{arom,ipso}$N); 159.7 (C(1,5)); 179.5 (C═N). ^{19}F NMR (CD_2Cl_2): δ −81.60 (s, 3 F, OTf); −80.76 (s, 3 F, OTf). Anal. Calcd for $C_{28}H_{30}F_6N_3O_6RhS_2$: C, 42.81; H, 3.85; N, 5.35. Found: C, 42.86; H, 3.94; N, 4.95. IR (CD_2Cl_2, triflate range): 1328 (OTf, covalent); 1293 (OTf, ionic); 1211 cm^{-1} (s, OTf, covalent).

Synthesis of the Rhodium(III) Methyl Bis(triflate) Complex 14. To a solution of 37 mg (60 μmol) of **11** in 2 mL of $C_2H_4Cl_2$ was added 39.6 μL (360 μmol) of MeOTf, yielding an orange solution, which was stirred for 36 h at room temperature. The reaction was evaporated to dryness under vacuum, and the solid remainder was washed with pentane (2 × 5 mL) to remove traces of excess MeOTf. Recrystallization from dichloromethane/pentane at −35 °C yielded 36 mg (42.8 μmol, 71%) of **14**. ^{1}H NMR (CD_2Cl_2): δ 1.53 (s, 9 H, C(CH$_3$)$_3$); 1.89 (d, ^2J(Rh,H) = 2 Hz, 3 H, Rh−C*H*$_3$); 2.13 (s, 6 H, CN−CH$_3$); 2.43 (s, 6 H, CH$_3$); 2.46 (s, 6 H, CH$_3$); 7.11−7.21 (m, 6 H, CH_{arom}); 7.98 (s, 2 H, CH(2,4)). ^{13}C{^{1}H} NMR (CD_2Cl_2): δ 4.5 (Rh−CH$_3$); 19.0 (CH$_3$); 19.1 (CN−*C*H$_3$); 19.9 (CH$_3$); 30.5 (C(*C*H$_3$)$_3$); 36.9 (*C*(CH$_3$)$_3$); 125.8 (CH(2,4)); 128.4, 129.0, 130.4 (C_{arom}H); 133.7 (*C*$_{arom,ipso}$CH$_3$); 143.5 ($C_{arom,ipso}$N); 159.0 (C(1,5); 166.8 (C(3)); 179.8 (C═N). ^{19}F NMR (CD_2Cl_2): δ −80.71 (s, 3

F, OTf); −81.60 (s, 3 F, OTf). Anal. Calcd for $C_{32}H_{38}N_3F_6O_6RhS_2$: C, 45.60; H, 4.55; N, 4.99. Found: C, 45.65; H, 4.73; N, 5.14.

Synthesis of the Iridium(III) Methyl Bis(triflate) Complex 15. To a solution of 124 mg (207 μmol) of complex **7** in 8 mL of $C_2H_2Cl_4$ was added 114 μL (1.03 mmol) of MeOTf. The mixture was stirred for 2 h; during this time MeCl formed in the reaction was removed by applying a weak vacuum three times. The solvent was then removed in vacuo and the solid recrystallized from a mixture of CH_2Cl_2 and pentane at −35 °C. This yielded 111 mg (127 μmol) (61%) of **15** as dark green, almost black crystals. ^{1}H NMR (CD_2Cl_2): δ 1.13 (s, 3 H, Ir−CH_3); 2.17 (s, 6 H, CH_3); 2.44 (s, 6 H, CH_3), 2.85 (s, 6 H, CN−CH_3); 7.18−7.27 (m, 6 H, CH_{arom}); 7.99 (s, 3 H, CH(2,3,4)). ^{13}C{^{1}H} NMR (CD_2Cl_2): δ 14.2 (Ir−CH_3); 18.4 (CN−CH_3); 19.6 (broad, CH_3); 127.4 (CH(2,4) or CH(3)); 128.5, 129.2, 130.4 ($C_{arom}H$); 133.6 ($C_{arom,ipso}CH_3$); 138.7 (CH(2,4) or CH(3)); 144.4 ($C_{arom,ipso}N$); 162.8 (C(1,5)); 183.5 (C═N). ^{19}F NMR (CD_2Cl_2): δ −80.6 (s, 3 F, OTf); −81.3 (s, 3 F, OTf). Anal. Calcd for $C_{28}H_{30}F_6IrN_3O_6S_2$: C, 38.44; H, 3.46; N, 4.80. Found: C, 38.06; H, 3.42; N, 4.73.

Synthesis of the Rhodium Complex 16·dme. A solution of 961 mg (1.44 mmol) of **17** in 10 mL of dme was degassed in a high-vacuum Teflon tap (Young) sealed Schlenk tube by a freeze−pump−thaw (fpt) cycle and then heated under vacuum to 100 °C. After 1 day the solvent was evaporated under high vacuum, the solid residue was redissolved in dme, and the solution was degassed (fpt cycle) and heated again to 100 °C. This procedure was repeated three times; the total duration was 5 days. After removal of the solvent under high vacuum, the residual brown microcrystalline powder was washed with pentane (2 × 5 mL) and finally dried in vacuo, yielding 995 mg (1.4 mmol), 97%, of the analytically pure product **16**·dme. ^{1}H NMR (THF-d_8): δ 2.01 (s, 6 H, CN−CH_3); 2.32 (s, 12 H, CH_3); 3.29 (s, dme); 3.49 (s, dme); 7.16 (s, 6 H, CH_{arom}); 8.12 (d, ^3J = 8 Hz, 2 H, CH(2,4)); 8.45 (t, ^3J = 8 Hz, 1 H, CH(3)). ^{13}C{^{1}H} NMR (THF-d_8): δ 16.7 (CN-CH_3); 18.4 (CH_3); 59.1, 72.9 (dme); 127.5 (CH(2,4) and $C_{arom}H$); 129.6 (C_{arom} H); 131.1 (CH(3)); 132.8 ($C_{arom,ipso}CH_3$); 148.2 ($C_{arom,ipso}N$); 158.8 (C(1,5)); 172.7 (C═N). ^{19}F NMR (THF-d_8): δ −80.9 (s, OTf). IR (OTf range, CD_2Cl_2): 1317 (s), 1211 (s) cm^{-1} (covalent OTf, tentative, see text). Anal. Calcd for $C_{30}H_{37}N_3F_3O_5RhS$: C, 50.64; H, 5.24; N, 5.90. Found: C, 50.90; H, 5.58; N 5.82.

Synthesis of the Rh(I) Ethylene Complex 17. To a solution of 646 mg (1.66 mmol) of $[Rh(C_2H_4)_2Cl]_2$ in 20 mL of THF and 5 mL of diethyl ether was added slowly a solution of 853 mg (3.32 mmol) of AgOTf in 15 mL of THF with vigorous stirring. The yellow suspension was stirred for 5 min and stored at −35 °C for 20 min. The precipitated AgCl was removed by centrifugation; the supernatant yellow solution was filtered and then reduced in vacuo to 20 mL. The concentrated dark orange solution was filtered again to remove further traces of AgCl. To this filtrate was added slowly a solution of 1.228 g (3.32 mmol) of ligand **A** in a mixture of 10 mL diethyl ether and 5 mL of THF, yielding a dark brown solution which was stirred for 1 h, upon which the formation of a dark green (sometimes brown) microcrystalline precipitate was observed. The solvent was reduced to 20 mL in vacuo, and then 10 mL diethyl ether was added to complete precipitation of the product. The supernatant solvent was decanted off, and the solid was dried under high vacuum, washed with pentane (2 × 10 mL), and finally dried under high vacuum. This yielded 2.26 g (3.13 mmol, 94%) of **17** as an analytically pure green microcrystalline solid. ^{1}H NMR (CD_2Cl_2): δ 1.81 (m, $^1/_4$ THF); 1.95 (s, 6 H, CN−CH_3); 2.18 (s, 12 H, CH_3); 3.39 (d, ^3J(Rh,H) = 2 Hz, 4 H, C_2H_4); 3.68 (m, $^1/_4$ THF); 7.12 (s, 6 H, CH_{arom}); 8.04 (d, ^3J = 8 Hz, 2 H, CH(2,4)); 8.32 (t, ^3J = 8 Hz, 1 H, CH(3)). ^{13}C{^{1}H} NMR (CD_2Cl_2): δ 17.3 (CN−CH_3); 17.9 (CH_3); 25.9 (THF); 68.1 (THF); 78.7 (d, ^1J(Rh,C) = 11 Hz, C_2H_4); 126.2 (CH(2,4)); 127.5, 128.3, 129.1 ($C_{arom}H$); 142.0 (CH(3)); 143.6 ($C_{arom,ipso}N$); 156.2 (C(1,5)); 175.5 (C═N). ^{13}C NMR: Rh(C_2H_4) resonance, δ 78.7 (dt, ^1J(C,H) = 158 Hz, ^1J(Rh,C) = 11 Hz). ^{19}F NMR (THF-d_8): δ −80.87 (s, OTf). IR (imine range, CH_2Cl_2): 1593 (m, C═N) cm^{-1}. Anal. Calcd for $C_{29}H_{33}N_3F_3O_{3.25}RhS$ (**17**·0.25 THF): C, 52.18; H, 4.98; N, 6.29. Found: C, 52.41; H, 5.02; N, 5.96. The presence of $^1/_4$ molecule of THF per molecule of **17** in the crystalline material was confirmed by ^{1}H NMR integration of several batches.

Synthesis of the Rh(III) Ethyl Bis(triflate) Complex 18. To 35 mg (48 μmol) of **17** dissolved in 5 mL of dichloromethane was added 4.7 μL (53 μmol) of HOTf, upon which a color change from dark brown to orange was noticed. After the solution was stirred for 1.5 h, the solvent was reduced to half in vacuo and layered with pentane. Crystallization of this mixture at −35 °C yielded 16 mg (19 μmol, 40%) of **18** as red crystals. Crystals suitable for X-ray diffraction were also obtained in this way. ^{1}H NMR (CD_2Cl_2): δ 0.29 (t, ^3J = 8 Hz, 3 H, Rh−CH_2−CH_3); 2.19 (s, 6 H, CH_3); 2.44 (s, 6 H, CH_3); 2.48 (s, 6 H, CN−CH_3); 3.30 (dq, ^2J(Rh,H) = 3 Hz, ^3J = 8 Hz, 2 H, Rh−CH_2−CH_3); 7.13−7.22 (m, 6 H, CH_{arom}); 8.05 (d, ^3J = 8 Hz, 2 H, CH(2,4)); 8.36 (t, ^3J = 8 Hz, 1 H, CH(3)). ^{13}C{^{1}H} NMR (CD_2Cl_2): δ 18.1 (Rh−CH_2−CH_3); 18.7 (CH_3); 18.8 (CN−CH_3); 20.2 (CH_3); 21.4 (d, ^1J(Rh,C) = 24 Hz, Rh−CH_2CH_3); 128.4 (C_{arom} H), 128.7 (CH(2,4)); 129.0, 130.6 ($C_{arom}H$); 133.8 ($C_{arom,ipso}CH_3$); 140.1 (CH(3)); 143.4 ($C_{arom,ipso}N$); 159.4 (C(1,5)); 179.7 (C═N). ^{19}F NMR (CD_2Cl_2): δ −80.6 (s, 3 F, OTf); −81.6 (s, 3 F, OTf). Anal. Calcd for $C_{29}H_{32}N_3F_6O_6RhS_2$: C, 43.56; H, 4.03; N, 5.26. Found: C, 43.71; H, 4.09; N, 5.27.

Synthesis of the Rhodium(I) BH_4 Complex 19. A mixture of 118 mg (165 μmol) of **16**·dme and 6.5 mg (172 μmol) of $NaBH_4$ was suspended in 10 mL of THF, which was stirred for 10 min, upon which a color change from brown to green-blue was observed. The solvent was removed in vacuo, leaving a solid remainder, which was washed with 10 mL of pentane and then dried under high vacuum. The product was extracted into diethyl ether, filtered, and evacuated to dryness. It was dissolved in a small amount of THF and recrystallized from a solvent mixture of diethyl ether and pentane at −35 °C, yielding **19** as dark green, analytically pure crystals. Yield: 41 mg (84 μmol), 51%. ^{1}H NMR (C_6D_6, 298 K): δ 1.25 (s, 6 H, CN−CH_3); 2.06 (s, 12 H, CH_3); 7.02−7.07 (m, 6 H, CH_{arom}); 7.12 (d, ^3J = 8 Hz, 2 H, CH(2,4)); 7.40 (t, ^3J = 8 Hz, 1 H, CH(3)). The signals of the BH_4 group could not be detected at this temperature. In the ^{1}H NMR spectrum at −100 °C in THF-d_8 a broad pseudo-doublet at −5.82 ppm (^1J(B,H) = 40 Hz) was observed for the BH_4 group. ^{13}C{^{1}H} NMR (C_6D_6): δ 15.9 (CN−CH_3), 18.8 (CH_3); 116.2 (CH(3)); 124.7 (CH(2,4)); 126.1, 129.9 ($C_{arom}H$); 148.5, 148.6, 149.3 ($C_{arom,ipso}N$, $C_{arom,ipso}$-CH_3, C(1,5)); 163.8 (C═N). Anal. Calcd for $C_{25}H_{31}N_3BRh$: C, 61.63; H, 6.41; N, 8.62. Found: C, 61.30; H, 6.33; N, 8.44. IR (KBr, B−H range): 2405 (s), 2363 (s) (B−H terminal); 1914 (w), 1901 (vw) (B−H bridging) cm^{-1}. IR (BD_4 isotopomer): 1828 (w), 1811 (s) (B−D terminal); 1740 (vs) (B−D bridging) cm^{-1}. Single crystals suitable for X-ray diffraction were obtained by slow diffusion of pentane into a solution of **19** in diethyl ether at room temperature.

Synthesis of the Rh(I) Methoxide Complex 20. A solution of 42 mg (72 μmol) of the rhodium chloro complex **4** in 5 mL of MeOH and 5 mg (87 μmol) of NaOMe was stirred for 30 min. The reaction mixture was evaporated to dryness, the remaining green solid washed with pentane (2 × 5 mL), and the product finally extracted into toluene. The toluene fraction was filtered, the solvent was removed under high vacuum, and the obtained dark green solid was washed with pentane (2 × 5 mL) and then dried under high vacuum, yielding 35 mg (70 μmol, 96%) of **20** as a dark green analytically pure compound. ^{1}H NMR (C_6D_6): δ 1.00 (s, 6 H, CN−CH_3); 2.14 (s, 12 H, CH_3); 4.47 (s, 3 H, OCH_3); 6.98−7.06 (m, 6 H, CH_{arom}); 7.12 (d, ^3J = 8 Hz, 2 H, CH(2,4)); 7.80 (t, ^3J = 8 Hz, 1 H, CH(3)). ^{13}C{^{1}H} NMR (C_6D_6): δ 17.1 (CN−CH_3); 19.2 (CH_3); 61.2 (OCH_3); 116.4 (CH(3)); 124.9 (CH(2,4)), 126.0, 128.9 ($C_{arom}H$); 131.0 ($C_{arom,ipso}CH_3$), 150.5 ($C_{arom,ipso}N$); 155.2 (d,

^2J(Rh,*C*) = 2.6 Hz, C(1,5)); 163.4 (C═N). Anal. Calcd for $C_{26}H_{30}N_3ORh$: C, 62.03; H, 6.01; N, 8.35. Found: C, 62.32; H, 6.34; N, 8.45.

Synthesis of the Ir(I) Methoxide Complex 21. To a vigorously stirred solution of 105 mg (176 μmol) of **7** in 20 mL of MeOH was added slowly a solution of 15 mg (278 μmol) of NaOMe in 8 mL of MeOH, and the mixture was allowed to react for 30 min. The solvent was removed in vacuo, washed with pentane (3 × 5 mL), and dried again under high vacuum. The crude reaction product was extracted into toluene, the extract was centrifuged and filtered, the filtrate was evaporated to dryness in vacuo, and the brown solid residue was washed with pentane (2 × 5 mL). Drying under high vacuum yielded 92 mg (155 μmol, 88%) of complex **21** as an analytically pure brown solid. ^{1}H NMR (C_6D_6): δ 0.42 (s, 6 H, CN−CH_3); 2.06 (s, 12 H, CH_3); 5.45 (s, 3 H, OCH_3); 7.01−7.07 (m, 6 H, CH_{arom}); 7.73 (d, ^3J = 8 Hz, 2 H, CH(2,4)); 7.92 (t, ^3J = 8 Hz, 1 H, CH(3)). ^{13}C{^{1}H} NMR (C_6D_6): δ 18.6 (CH_3); 19.1 (CN−*C*H_3); 67.6 (OCH_3); 115.1 (CH(3)); 122.1 (CH(2,4)); 126.2, 128.5 (C_{arom}H); 130.9 ($C_{arom,ipso}CH_3$); 154.1 ($C_{arom,ipso}$N); 160.1 (C(1,5)), 165.0 (C═N). Anal. Calcd for $C_{26}H_{30}N_3OIr$: C, 52.68; H, 5.10; N, 7.09. Found: C, 52.82; H, 5.41; N, 6.90. Crystals suitable for X-ray diffraction were obtained from a solution of **21** in toluene layered with pentane at −35 °C.

Synthesis of the Rh(I) Methyl Complex 22. A 57 μL portion of MeMgCl (3 M in THF) was added to a solution of 86 mg (171 μmol) of **20** in 10 mL of toluene, and the mixture was stirred for 20 min. The solvent was removed in vacuo and the solid residue washed with pentane (2 × 5 mL) and then dried again under high vacuum. The dark green solid was extracted into diethyl ether, the extract was filtered through a glass frit, and the solvent was evaporated to dryness under high vacuum, yielding 58 mg (119 μmol, 70%) of **22** as an analytically pure, green compound. ^{1}H NMR (C_6D_6): δ 0.70 (s, 6 H, CN−CH_3); 2.09 (s, 12 H, CH_3); 2.21 (d, ^2J(Rh,H) = 1 Hz, 3 H, Rh−CH_3); 7.04−7.10 (m, 6 H, CH_{arom}); 7.31 (d, ^3J = 8 Hz, 2 H, CH(2,4)); 8.16 (t, ^3J = 8 Hz, 1 H, CH(3)). ^{13}C{^{1}H} NMR (C_6D_6): δ 0.2 (d, ^1J(Rh,C) = 33 Hz, Rh−CH_3); 18.0 (CN-*C*H_3); 19.3 (CH_3); 121.7 (CH(3)); 123.4 (CH(2,4)); 125.5 (C_{arom}H); 130.2 ($C_{arom,ipso}CH_3$); 151.4 ($C_{arom,ipso}$N); 155.2 (C(1,5)); 165.5 (C═N). One of the aromatic C−H resonances of the 2,6-dimethyl-substituted phenyl ring could not be detected; presumably it is obscured by the resonance of the C_6D_6 solvent. Anal. Calcd for $C_{26}H_{30}N_3Rh$: C, 64.07; H, 6.20; N, 8.62. Found: C, 64.26; H, 6.09; N, 8.47.

Synthesis of the Ir(I) Methyl Complex 23. To a solution of 182 mg (307 μmol) of **21** in 6 mL of THF was added 10 μL (102 μmol) of neat $AlMe_3$. The solvent was removed in vacuo, the remaining solid was extracted into diethyl ether, and finally the solvent was evaporated to dryness, leaving a green solid material. Although the yield of the reaction appears to be essentially quantitative (on the basis of the ^{1}H NMR spectrum of the crude reaction mixture), the isolation of pure **23** is somewhat cumbersome. This is due to the sensitivity of the product, which restricts the purification process solely to recrystallization (decomposition was observed in chromatography attempts on alumina and silica support). Unfortunately, in large-scale reactions, we have not found sufficiently good conditions to remove residual small traces of aluminum-containing species. An analytically pure sample (smaller amount) was obtained by crystallization of a large reaction scale batch. The ^{1}H NMR spectrum of this sample proved to be identical with that for **23** observed in the crude mixture. Crystals suitable for X-ray diffraction were obtained from a saturated solution of **23** in pentane at −35 °C. ^{1}H NMR (THF-d_8): δ 0.21 (s, 6 H, CN−CH_3); 1.96 (s, 12 H, CH_3); 6.91 (s, 3 H, Ir−CH_3); 7.02−7.18 (m, 6 H, CH_{arom}); 8.40 (d, ^3J = 8 Hz, 2 H, CH(2,4)); 8.91 (t, ^3J = 8 Hz, 1 H, CH(3)). ^{13}C{^{1}H} NMR (THF-d_8): δ 2.7 (Ir−CH_3); 18.5 (CH_3), 20.9 (CN−*C*H_3), 120.7 (CH-(2,4)); 123.5 (CH(3)); 126.0, 128.2 (C_{arom}H), 130.8 ($C_{arom,ipso}CH_3$), 156.1 ($C_{arom,ipso}$N); 163.7 (C(1,5)); 170.2 (C═N). Anal. Calcd for $C_{26}H_{30}N_3Ir$: C, 54.14; H, 5.24; N, 7.29. Found: C, 54.61; H, 5.21; N, 6.86.

Chart 2

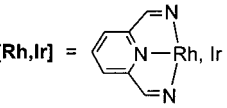

DFT Calculations. The DFT calculations were performed with the Turbomole program suite[61] and using the BP-86 functional[62,63] in its RI-DFT implementation[64] for the geometry optimizations and the calculation of the second derivatives. As tested for a few cases, essentially identical energy differences were obtained with the BP-86 functional using the *pure* DFT BP86 implementation rather than the RI-DFT method. The parallel version of the Turbomole program package was used on our 22 CPU Linux cluster in all cases. Initially, the geometries were optimized using a TZVP basis[65] with scalar-relativistic Stuttgart−Dresden ECPs[66] applied for the rhodium and iridium centers and SVP basis sets[67] for the residual atoms. After convergence (gradients $<10^{-3}$ hartree/bohr), a TZVP basis was applied for all atoms and the geometry optimization continued. Usually, this took just a few cycles to converge. Second derivatives were calculated by finite differences and were used to identify the optimized geometries as stationary points through the absence of imaginary frequencies. The Rh and Ir model fragment, [Rh,Ir], used in the calculation of the complexes is shown in Chart 2.

Final total energies $E_{tot,SCF}$ in hartrees with unscaled zero point energies (ZPEs) in parentheses for the optimized geometries using a Becke−Perdew (BP86) functional (RI-DFT method), TZVP basis sets for all atoms, and scalar-relativistic Stuttgart−Dresden pseudopotentials (ECP-28-mwb and ECP-60-mwb) for the Rh and Ir centers are as follows: CH_2O, −114.554 57(67.5); C_2H_4, −78.616 79(0.049 83); BH_3, −26.606 77 (0.025 73); quinuclidine, −329.425 69 (0.189 29); BH_3·quinuclidine, −356.095 24 (0.222 61); acetone, −193.234 89 (0.081 66) ; [Rh](κ^2-BH_4), **I**, −573.362 632 (0.170 08); [Rh]−H, **II**, −546.674 99 (0.138 28); [Rh]−OMe, **III**, −661.286 30 (0.171 79); [Rh]−O^{i}Pr, −739.949 20 (0.226 62); [Rh]−Et, **III**, −625.331 22 (0.193 22); [Ir]−H, **II**, −540.513 29 (0.138 55); [Ir]−OMe, **III**, −655.122 53 (0.171 91); [Ir]−OMe$^{\#}$, **III**$^{\#}$ (TS in Figure 9), 655.105 28 (0.170 95), +11 kcal mol^{-1} (one imaginary frequency, ν_{imag} = −300 cm^{-1}). For the Rh methoxy and hydride compounds, we have also performed geometry optimizations using the B3LYP hybrid functional,[68] which led to the following total energies (ZPEs in parentheses) for the optimized geometries and essentially identical reaction energies: [Rh]−H, **II**, -546.207 44 (0.140 95), [Rh]−OMe, **III**, −660.750 65 (0.176 71) [hartrees]. The reaction energies ΔE presented in Schemes 7 and 9 were calculated using the total energies E_{tot} given above corrected by their zero-point energies (E_{tot} = $E_{tot,SCF}$ + ZPE) and using $\Delta E = \sum \Delta E_{tot,products} - \sum \Delta E_{tot,starting\ material}$. In addition, the geometries of the methoxide complex **20** and its corresponding hydride compound were optimized using the BP86 functional (RI-DFT implementation), with TZVP basis sets for all atoms and a Stuttgart−Dresden ECP for the rhodium center. Because of the size of these systems, second derivatives were not calculated. Final

(61) Ahlrichs, R.; Bär, M.; Häser, M.; Horn, H.; Kölmel, C. *Chem. Phys. Lett.* **1989**, *162*, 165.
(62) Becke, A. D. *Phys. Rev. A* **1988**, *38*, 3098.
(63) Perdew, J. P. *Phys. Rev. B* **1986**, *33*, 8822.
(64) Eichkorn, K.; Treutler, O.; Oehm, H.; Häser, M.; Ahlrichs, R. *Chem. Phys. Lett.* **1995**, *242*, 652.
(65) Schäfer, A.; Huber, C.; Ahlrichs, R. *J. Chem. Phys.* **1994**, *100*, 5829.
(66) Andrae, D.; Häubermann, U.; Dolg, M.; Stoll, H.; Preub, H. *Theor. Chim. Acta* **1990**, *77*, 123.
(67) Schäfer, H.; Horn, H.; Ahlrichs, R. *J. Chem. Phys.* **1992**, *97*, 1992.
(68) Becke, A. D. *J. Chem. Phys.* **1993**, *98*, 5648.

total energies in hartrees (Cartesian gradients $<5 \times 10^{-4}$ hartree/bohr) are as follows: [Rh]−H −1 244.910 573; [Rh]−OMe, **20**, −1 359.518 54.

X-ray Crystal Structure Analyses. Suitable single crystals were mounted on glass fibers in polyisobutylene oil and transferred on the goniometer head to the diffractometer and the crystal cooled to −90 °C under a N_2 cryostream. The data sets were collected with graphite-monochromated Mo Kα radiation (0.707 173 Å) on a Stoe IPDS image plate diffractometer. Intensities were corrected for Lorentz and polarization effects and absorption corrections performed numerically with the faces and corresponding crystal dimensions determined using the STOE Faceit-Video CCD camera microscope system. The structures were solved using direct methods with the SHELX-97 program package.[69] The refinements were carried out with SHELXL-97 using all unique F_o^2 values.[69] All non-hydrogen atoms were refined anisotropically. Except for complex 19 the positions of the hydrogen atoms were calculated in idealized positions (C−H bonds fixed at 0.96 Å) and refined as a riding model. For complex 19, the hydrogen atoms of the Rh−BH_4 moiety were located in the difference Fourier map and were refined isotropically. The absolute configuration of 19 was confirmed by a Flack *x* parameter of −0.043(0.019) and 1.03(0.02) for the inverted structure. The details of the data collection and refinement, including *R* values, are summarized in Table 1.

(69) Sheldrick, G. M. SHELXL 97; University of Göttingen, Göttingen, Germany, 1997.

Acknowledgment. We are indebted to Prof. Heinz Berke for his generous support. We thank Dr. Thomas Fox for recording the $^{15}N-^{1}H$ NMR HMBC spectrum. Support of this work by the Swiss National Science Foundation is gratefully acknowledged.

Supporting Information Available: 2-D $^{15}H-^{1}H$ HMBC spectrum of the Ir methyl complex **23** and tables and figures giving X-ray crystallographic data for **4**, **11**, **13**, **18**, **19**, and **21**. This material is available free of charge via the Internet at http://pubs.acs.org.

OM010185Y